

Resonant grazing bifurcations revisited.

David J.W. Simpson¹ and Indranil Ghosh²

¹School of Mathematical and Computational Sciences, Massey University,
Palmerston North, New Zealand

²School of Mathematics and Statistics, University College Dublin, Dublin,
D04 V1W8, Ireland

February 27, 2026

Abstract

In vibro-impact mechanics, the division between an impact and a near miss is a zero-velocity grazing event. Grazing bifurcations of stable periodic motions often produce complicated attractors when grazing generates a square-root term in the Poincaré map. This paper concerns codimension-two scenarios for which the square-root term vanishes in some iterate of the Poincaré map. For forced one-degree-of-freedom oscillators, this occurs when the forcing frequency is a certain rational multiple of the damped natural frequency, i.e. the system is in resonance. In two-parameter bifurcation diagrams, curves of saddle-node and period-doubling bifurcations of single-impact periodic motions emanate from the codimension-two points. In this paper we prove these curves are quadratically tangent to the curve of grazing bifurcations, and derive explicit formulas for their quadratic coefficients. This is achieved by modifying the Poincaré map in a way that circumvents the square-root singularity, enabling us to use the implicit function theorem to demonstrate smoothness and perform asymptotic calculations of the saddle-node and period-doubling bifurcation curves. In doing so we resolve a long-standing conjecture on the admissibility of single-impact periodic motions by supplementing raw asymptotic computations with geometric and topological arguments. We illustrate the results with a linear impact oscillator model, matching the theoretical unfolding to numerically computed bifurcation curves. The results explain why previously reported physical experiments reveal an absence of chaos shortly past the grazing bifurcation.

1 Introduction

Many mechanical systems contain components that collide. Examples include vibro-impact capsules [1, 2], atomic force microscopes [3, 4], rotors [5, 6], gear assemblies [7, 8], and church

bells [9]. Each of these examples have interesting and physically relevant nonlinear dynamics caused by impact events.

To understand such dynamics we use a model. If the mechanical components are rigid, it is reasonable to use a *hybrid model* that combines ODEs (ordinary differential equations) for the motion between impacts, with one or more maps that capture impact events by accounting for velocity reversal, energy loss, impact duration, etc. [10–13]. In the phase space of the model, a map is applied when a trajectory reaches the corresponding *impacting surface*, Fig. 1.

The situation that demarcates a near miss from an impact, is an impact at which the velocity of the two objects relative to one another is zero. In phase space, this corresponds to a trajectory arriving at an impacting surface tangentially. When this occurs for a periodic solution, it is referred to as a *grazing bifurcation*. Grazing bifurcations often only alter the paths of trajectories locally, so cause the periodic solution to be replaced by an attractor located near this solution. If the attractor is periodic, it must consist of some $p \geq 1$ loops near the original periodic solution, and usually only one of these loops corresponds to an impact. Chin *et al.* [14] refer to such solutions as *maximal*. Here we call them p -loop MPSs (maximal periodic solutions).

Fig. 2 shows a typical example. As the value of the parameter \mathcal{A} is increased, a grazing bifurcation occurs when $\mathcal{A} = \mathcal{A}_{\text{graz}} \approx 0.2728$. This bifurcation generates p -loop MPSs for $p = 1, 2, 3$. For $p = 1$ and $p = 2$, these emanate to the right of the bifurcation, while for $p = 3$, the periodic solution emanates to the left of the bifurcation. The three solutions are all unstable as they emanate from the grazing bifurcation, but the two-loop MPS later gains stability in a period-doubling bifurcation, while the three-loop MPS later gains stability in a saddle-node bifurcation.

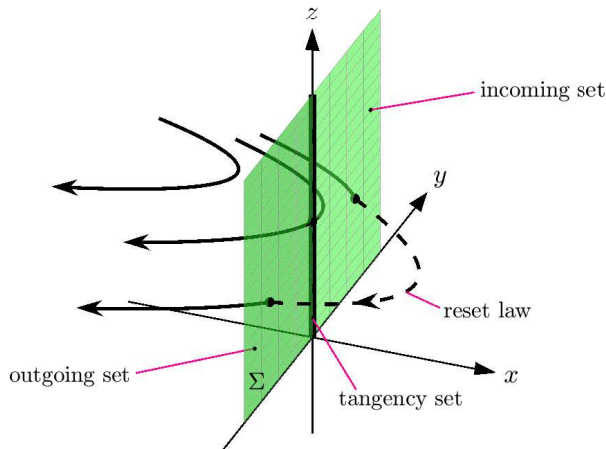


Figure 1: A sketch of phase space for the class of impacting hybrid systems introduced in §2. Orbits (solid curves) obey the ODEs until reaching the impacting surface Σ where they are mapped under the reset law. The impacting surface is partitioned into an incoming set, an outgoing set, and a tangency set, as determined by the direction of the ODEs relative to the surface. The reset law maps the incoming set to the outgoing set, and is the identity map on the tangency set.

To analyse the near-grazing dynamics, we study a Poincaré map. The stability of a p -loop MPS is determined by the eigenvalues of the Jacobian matrix of the p^{th} iterate of this map evaluated at one point of the solution. Nordmark [15] showed that for a broad class of impacting hybrid systems, such maps contain a square-root singularity. Due to the square-root singularity, the Jacobian matrix contains a term that tends to infinity at the grazing bifurcation. Consequently the p -loop MPS is unstable in a neighbourhood of the bifurcation.

However, there are codimension-two scenarios at which the coefficient of the singular term vanishes, and this is sufficient to stabilise the p -loop MPS as it emanates from the grazing bifurcation. This phenomenon was first explored by Ivanov [16] for $p = 1$ in a linear impact oscillator model. Ivanov argued that the one-loop MPS loses stability along curves of saddle-node and period-doubling bifurcations that emanate quadratically from the corresponding curve of grazing bifurcations. Foale [17] performed a similar analysis of the same problem and calculated the saddle-node and period-doubling curves to leading order, while Peterka [18] computed the saddle-node and period-doubling curves numerically. Kundu *et al.* [19, 20] rediscovered the phenomenon and showed that bifurcation diagrams of a truncated Poincaré map show an absence of chaos.

Later Dankowicz and Zhao [21, 22] treated the case $p = 1$ in a model of a micro-actuator and showed that leading-order theoretical expressions for the saddle-node and

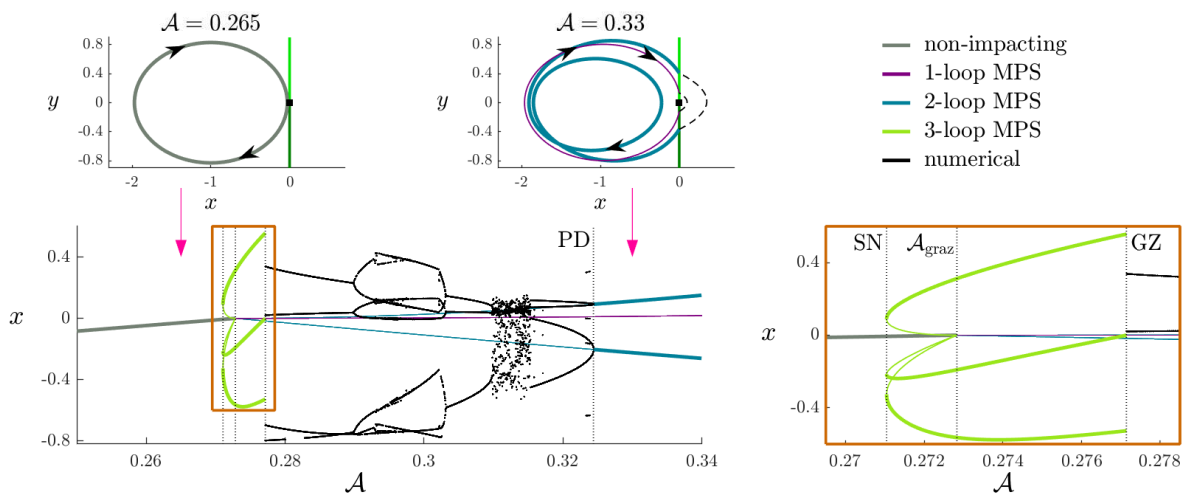


Figure 2: A bifurcation diagram of the linear impact oscillator model (3.1)–(3.2) with $\zeta = 0.02$, $\epsilon = 0.9$, and $\omega = 0.854$. The horizontal axis uses the forcing amplitude \mathcal{A} , while the vertical axis uses the x -value of P_{global} (so points with $x > 0$ indicate the occurrence of an impact). The right plot is a magnification; the upper plots are phase portraits. Branches of p -loop MPSs were computed by numerical continuation, and are indicated with thick curves where the solutions are stable, and thin curves where they are unstable. Four bifurcations are labelled: $\mathcal{A}_{\text{graz}}$: grazing bifurcation of the non-impacting periodic solution; PD: period-doubling bifurcation of the two-loop MPS; SN: saddle-node bifurcation of the three-loop MPS; GZ: grazing bifurcation of the three-loop MPS. Between GZ and PD we overlay a numerical bifurcation diagram showing the long-term behaviour of forward orbits of random initial points.

period-doubling curves are consistent with numerical computations of these curves. More recently the codimension-two scenario with $p = 1$ has been observed in models of other mechanical systems [23–25].

Nordmark [26] and later Thota *et al.* [27] treated cases with $p \geq 2$. These works presented heuristic arguments that saddle-node and period-doubling curves emanate quadratically from the grazing curve. For forced linear oscillators the codimension-two scenarios arise when the forcing frequency is a certain rational multiple of the damped natural frequency [16, 26]. For this reason, the scenarios are referred to as *resonant grazing bifurcations*.

The purpose of this paper is to unfold the $p = 1$ and $p \geq 2$ cases rigorously and in a general setting. We consider a nonlinear one-degree-of-freedom oscillator $\ddot{x} = F(x, \dot{x}, t)$, where F is periodic in t , impacts are modelled by a reset law R , and dots denote differentiation with respect to time t . In order to prove that saddle-node and period-doubling curves exist and are smooth, we work with a modification of the Poincaré map referred to as the VIVID function [28]. This function uses \dot{x} as an input, instead of x , and consequently its derivative is non-singular.

As a first step to obtaining the results, we determine the side of the grazing bifurcation on which the p -loop MPS is created, as this is different on different sides of the codimension-two point. Conditions for this were derived by Nordmark [26], however, it was never proved that these conditions are sufficient because it is challenging to show that the p -loop MPS is *admissible*. By admissible, we mean that all of the computed points at which the p -loop MPS intersects the Poincaré section lie on the correct side of the switching manifold dividing impacts from near misses. Admissibility is necessary for MPSs to be valid solutions of the hybrid system. Below we show that Nordmark’s conditions are sufficient by combining asymptotic calculations with geometric and topological arguments.

The remainder of this paper is organised as follows. The main results are presented in §2. Theorems 2.2 and 2.3 treat generic grazing bifurcations and explain which side of the grazing bifurcation the p -loop MPSs are admissible. Theorems 2.4 and 2.5 treat resonant grazing bifurcations and provide leading-order expressions for the saddle-node and period-doubling bifurcation curves.

In §3 we illustrate the results with a prototypical model of linear impact oscillator using parameter values based on laboratory experiments reported by Pavlovskaja *et al.* [29]. Their experiments showed a stable two-loop MPS very shortly after a grazing bifurcation, and we can now conclude that this occurs because the bifurcation is close to $p = 2$ resonance. For resonant grazing bifurcations with $p = 1, 2,$ and 3 , we numerically continue saddle-node and period-doubling bifurcations, and compare these to the theoretical unfolding.

The four theorems are proved in Sections 4 and 5. Conclusions are presented in §6.

2 Main results

2.1 A general class of impacting hybrid systems

Let $x(t) \in \mathbb{R}$ denote the position of an object subject to a collection of forces. We write

$$\ddot{x} = F(x, \dot{x}, t; \mu, \eta), \tag{2.1}$$

where F is periodic in t with period $\frac{2\pi}{\omega(\mu,\eta)}$, and $\mu, \eta \in \mathbb{R}$ are parameters. To write (2.1) as an autonomous system, we let $y(t) = \dot{x}(t)$ denote the velocity of the object, and

$$z = \omega(\mu, \eta)t \bmod 2\pi, \quad (2.2)$$

denote the phase of F , which takes values in $[0, 2\pi)$. Then (2.1) can be written as

$$\begin{bmatrix} \dot{x} \\ \dot{y} \\ \dot{z} \end{bmatrix} = \begin{bmatrix} y \\ F(x, y, \frac{z}{\omega(\mu,\eta)}; \mu, \eta) \\ \omega(\mu, \eta) \end{bmatrix}. \quad (2.3)$$

Now suppose a wall is located at $x = 0$, and the object only obeys (2.3) for $x \leq 0$. The object may hit the wall; in (x, y, z) -phase space this occurs when an orbit reaches the *impacting surface*

$$\Sigma = \{(0, y, z) \mid y \in \mathbb{R}, z \in [0, 2\pi)\}.$$

Since $\dot{x} = y$, impacting events occur at points on Σ with $y > 0$, or with $y = 0$ in the special case that the impact velocity is zero. Consequently, we refer to the part of Σ with $y > 0$ as is the *incoming set*, the part of Σ with $y = 0$ as is the *tangency set*, and the part of Σ with $y < 0$ as is the *outgoing set*, Fig. 1. Since (2.3) applies for $x \leq 0$, grazing orbits have $\ddot{x} < 0$. For this reason we refer to the subset of the tangency set

$$\Sigma_{\text{graz}} = \left\{ (0, 0, z) \mid z \in [0, 2\pi), F(0, 0, \frac{z}{\omega(\mu,\eta)}; \mu, \eta) < 0 \right\},$$

as the *grazing set*.

With the viewpoint that the object and wall are rigid, we model impact events with a reset law R that updates the values of y and z . The only assumption we place upon R , besides smoothness, is that it converts a positive impact velocity to a negative recoil velocity, and leaves y and z unchanged when the impact velocity is zero. That is, R maps the incoming set to the outgoing set, and is the identity map on the tangency set. With this assumption, the reset law can be written as

$$R(y, z; \mu, \eta) = \begin{bmatrix} -y\Phi(y, z; \mu, \eta) \\ (z + y\Psi(y, z; \mu, \eta)) \bmod 2\pi \end{bmatrix}, \quad (2.4)$$

where Φ and Ψ are real-valued functions, and Φ takes only positive values.

In summary, the motion of the object is modelled by (2.3) for $x \leq 0$, and

$$\begin{bmatrix} y \\ z \end{bmatrix} \mapsto R(y, z; \mu, \eta), \quad \text{when } x = 0 \text{ with } y > 0, \quad (2.5)$$

where R has the form (2.4). Several research groups have formulated models of this form and found good agreement to the physically observed behaviour of simple impacting machines [30–33]. Often Φ is treated as a constant, in which case Φ is the coefficient of restitution. If $\Psi = 0$, then impacts are assumed to occur instantaneously.

In the above formulation, we have incorporated the parameters μ and η in a general manner so that they can be set equal to the forcing frequency, the coefficient of restitution, some other system parameter, or any shifted version of these so that the grazing bifurcation can be assumed to occur at $\mu = 0$, as in the theorems below.

2.2 Grazing and a global return map

We first describe typical grazing bifurcations, and to this end suppress the parameter η . For a grazing bifurcation at $\mu = 0$, we make the following assumption.

Assumption 2.1. Suppose (2.3) with $\mu = 0$ has a periodic solution Γ intersecting Σ at exactly one point $(0, 0, z_{\text{graz}}) \in \Sigma_{\text{graz}}$.

In order to state quantitative theorems, we consider the return map $(x', z') = P_{\text{global}}(x, z; \mu)$, defined as follows. Let $\Pi \subset \mathbb{R}^3$ be a compact part of the plane $y = 0$ in a neighbourhood of $(0, 0, z_{\text{graz}})$ that intersects Γ only at $(0, 0, z_{\text{graz}})$. For any $(x, 0, z) \in \Pi$, let $(x', 0, z')$ be the next point at which the forward orbit of $(x, 0, z)$ under (2.3) intersects Π , see Fig. 3. In a sufficiently small neighbourhood of $(x, z; \mu) = (0, z_{\text{graz}}; 0)$, the map P_{global} is smooth because impact events are ignored and orbits intersect Π transversally with a return time close to the period of Γ . Thus we can write

$$P_{\text{global}}(x, z; \mu) = \begin{bmatrix} 0 \\ z_{\text{graz}} \end{bmatrix} + A \begin{bmatrix} x \\ z - z_{\text{graz}} \end{bmatrix} + b\mu + \mathcal{O}((|x| + |z - z_{\text{graz}}| + |\mu|)^2), \quad (2.6)$$

where

$$A = DP_{\text{global}}(0, z_{\text{graz}}; 0) = \begin{bmatrix} \frac{\partial x'}{\partial x} & \frac{\partial x'}{\partial z} \\ \frac{\partial z'}{\partial x} & \frac{\partial z'}{\partial z} \end{bmatrix}, \quad (2.7)$$

$$b = \frac{\partial P_{\text{global}}}{\partial \mu}(0, z_{\text{graz}}; 0). \quad (2.8)$$

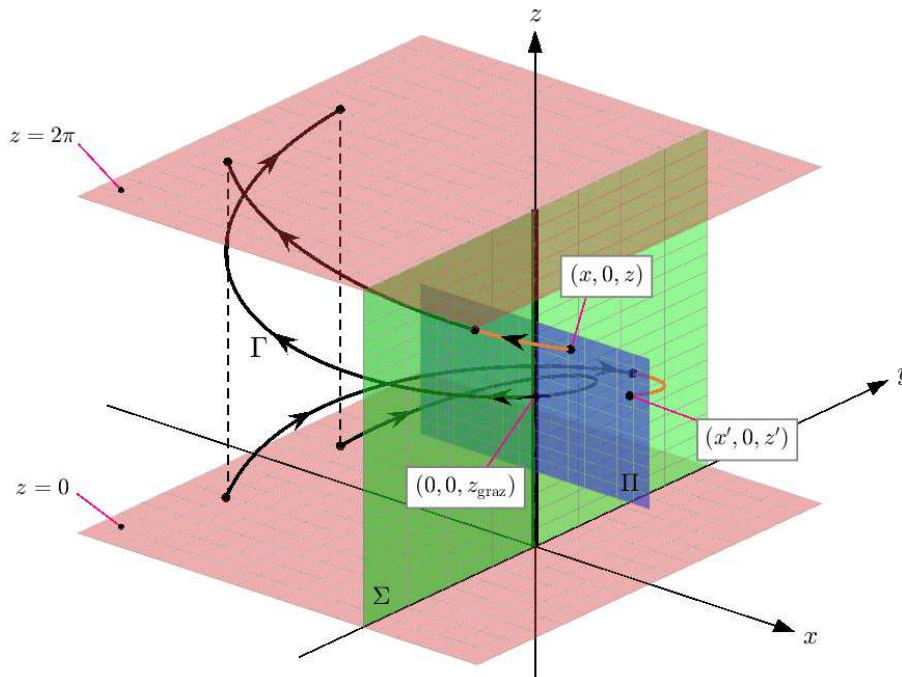


Figure 3: A sketch illustrating the P_{global} : the return map to Π induced by the flow of (2.3). We also sketch the grazing periodic solution Γ of Assumption 2.1.

2.3 Existence and stability of the non-impacting periodic solution

Let

$$\tau = \text{trace}(A), \quad \delta = \det(A). \quad (2.9)$$

If $\delta - \tau + 1 \neq 0$, then the matrix $I - A$ is non-singular and in a neighbourhood of $(x, z; \mu) = (0, z_{\text{graz}}; 0)$ the map P_{global} has the unique fixed point

$$\begin{bmatrix} x^*(\mu) \\ z^*(\mu) \end{bmatrix} = \begin{bmatrix} 0 \\ z_{\text{graz}} \end{bmatrix} + (I - A)^{-1}b\mu + \mathcal{O}(\mu^2). \quad (2.10)$$

With $\mu = 0$, this point corresponds to the grazing orbit Γ . If $x^*(\mu) < 0$, the fixed point corresponds to a non-impacting periodic solution of (2.3)–(2.5).

For each $i, j = 1, 2$, we let a_{ij} denote the (i, j) -entry of A , and b_i denote the i^{th} component of b . From (2.10),

$$\frac{dx^*}{d\mu}(0) = \frac{\beta}{\delta - \tau + 1}, \quad (2.11)$$

where

$$\beta = (1 - a_{22})b_1 + a_{12}b_2. \quad (2.12)$$

Thus $\beta \neq 0$ is the *transversality condition* for the grazing bifurcation. This ensures the non-impacting periodic solution collides with Σ in a generic fashion as μ is varied through 0.

Let

$$\lambda_1 = \frac{1}{2}(\tau + \sqrt{\tau^2 - 4\delta}), \quad \lambda_2 = \frac{1}{2}(\tau - \sqrt{\tau^2 - 4\delta}), \quad (2.13)$$

denote the eigenvalues of A . These are the stability multipliers (or non-trivial Floquet multipliers) associated with Γ when impact events are ignored, and are either real or complex conjugates of one another. Below we assume $|\tau| - 1 < \delta < 1$, so that Γ is asymptotically stable, in which case the non-impacting periodic solution is asymptotically stable for sufficiently small values of μ . Further, we assume P_{global} is orientation-preserving, so $\delta > 0$, as is usually the case in applications. Hence we restrict our attention to pairs (τ, δ) belonging to the trapezium

$$\mathcal{T} = \{(\tau, \delta) \in \mathbb{R}^2 \mid 0 < \delta < 1, |\tau| < \delta + 1\}, \quad (2.14)$$

shown in Fig. 4.

2.4 Maximal periodic solutions

The grazing bifurcation at $\mu = 0$ can give birth to a wide variety of invariant sets. Of these, we focus on p -loop MPSs (maximal periodic solutions) which consist of p loops near Γ and have exactly one impacting event. Theorems 2.2 and 2.3 explain which p -loop MPSs arise, and on which side of the grazing bifurcation they emerge.

The case $p = 1$ is straight-forward: in generic situations a one-loop MPS is always created and the side of the bifurcation on which it emerges is governed by the sign of a_{12} . To handle $p \geq 2$, we introduce some auxiliary functions. We first define

$$g_p(\delta) = 2\sqrt{\delta} \cos\left(\frac{\pi}{p}\right), \quad (2.15)$$

$$H_p(\tau, \delta) = \sum_{j=1}^{p-1} \sum_{k=1}^j \lambda_1^{k-j} \lambda_2^{1-k}, \quad (2.16)$$

where λ_1 and λ_2 are given by (2.13), and in (2.15) we allow non-integer values of p . We then define $h_2(\delta) = -2\sqrt{\delta}$, and for all $p \geq 3$ let $h_p(\delta)$ be the largest value of $\tau \in \mathbb{R}$ at which $H_p(\tau, \delta) = 0$. The following bounds on $h_p(\delta)$ are established in Appendix A.

Lemma 2.1. *For any $0 < \delta < 1$ and $p \geq 3$, we have $g_{\frac{p}{2}}(\delta) < h_p(\delta) < g_{p-1}(\delta)$.*

The curves $\tau = g_p(\delta)$ and $\tau = h_p(\delta)$ are shown in Fig. 4 for $p = 2, 3, \dots, 6$. As $p \rightarrow \infty$, the curves limit to $\tau = 2\sqrt{\delta}$. Nordmark [26] conjectured that if $g_p(\delta) < \tau < \delta + 1$, then a p -loop MPS emanates on one side of the bifurcation, while if $h_p(\delta) < \tau < g_p(\delta)$, then a p -loop MPS emanates on the other side of the bifurcation. Theorem 2.3 shows this to be true.

For example, the grazing bifurcation in Fig. 2 has $(\tau, \delta) \approx (0.8248, 0.7451)$, indicated by a star in Fig. 4. This point lies to the right of $\tau = g_2(\delta)$, thus a two-loop MPS emanates to the right of the grazing bifurcation. Also, $h_p(\delta) < \tau < g_p(\delta)$ for $p = 3, 4, 5$, thus a p -loop MPS emanates to the left of the grazing bifurcation for $p = 3, 4, 5$ (for clarity only the $p = 3$ solution is shown in Fig. 2). Theorem 2.3 does not handle values of p for which $\tau < h_p(\delta)$, indeed p -loop MPSs with $p = 5$ and $p \geq 7$ can arise for $(\tau, \delta) \in \mathcal{T}$ when $\delta \approx 1$ [26]. These solutions do not relate to resonant grazing, so we do not consider them in this paper.

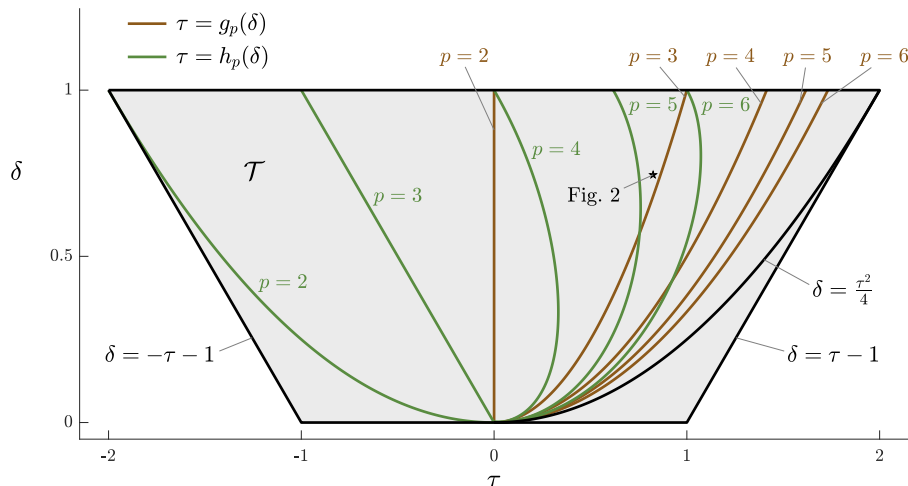


Figure 4: The curves $\tau = g_p(\delta)$ and $\tau = h_p(\delta)$ for $p = 2, 3, \dots, 6$ for values within the trapezium \mathcal{T} (2.14).

2.5 Unfolding generic grazing bifurcations

To account for the impact events neglected by P_{global} , we use a discontinuity map P_{disc} . As shown in §4.1, P_{disc} has a \sqrt{x} -term whose coefficient contains the factor

$$\alpha = 1 + \phi - \frac{\gamma\psi}{\omega(0)}, \quad (2.17)$$

where

$$\phi = \Phi(0, z_{\text{graz}}; 0), \quad \psi = \Psi(0, z_{\text{graz}}; 0), \quad \gamma = -F\left(0, 0, \frac{z_{\text{graz}}}{\omega(0)}; 0\right). \quad (2.18)$$

The sign of α is important to the dynamics created in the grazing bifurcation. Notice $\gamma > 0$, by the assumption that the grazing point belongs to Σ_{graz} .

Theorem 2.2 (generic grazing, $p = 1$). *Consider an impacting hybrid system (2.3)–(2.5) where F and R are C^3 , and $\eta \in \mathbb{R}$ is fixed. Suppose Assumption 2.1 holds, $(\tau, \delta) \in \mathcal{T}$, and $\alpha > 0$. A unique unstable one-loop MPS emanates from the grazing bifurcation for $\mu > 0$ if $a_{12}\beta > 0$, and for $\mu < 0$ if $a_{12}\beta < 0$.*

Now let $\kappa_p = \tau - g_p(\delta)$.

Theorem 2.3 (generic grazing, $p \geq 2$). *Consider an impacting hybrid system (2.3)–(2.5) where F and R are C^3 and $\eta \in \mathbb{R}$ is fixed, and let $p \geq 2$. Suppose Assumption 2.1 holds, $(\tau, \delta) \in \mathcal{T}$, $a_{12}\alpha > 0$, and $\tau > h_p(\delta)$. A unique unstable p -loop MPS emanates from the grazing bifurcation for $\mu > 0$ if $\beta\kappa_p > 0$, and for $\mu < 0$ if $\beta\kappa_p < 0$.*

2.6 Unfolding resonant grazing bifurcations

Theorem 2.2 shows that for $p = 1$, a codimension-two scenario arises when $a_{12} = 0$, while Theorem 2.3 shows that for $p \geq 2$, a codimension-two scenario arises when $\tau = g_p(\delta)$. To unfold these, we use the second parameter η and the following more general assumption that grazing occurs at $\mu = 0$ for all values of η in a neighbourhood $\mathcal{N} \subset \mathbb{R}$ of 0.

Assumption 2.2. Suppose that for all $\eta \in \mathcal{N}$, the system (2.3) with $\mu = 0$ has a periodic orbit Γ_η that varies continuously with η and intersects Σ at exactly one point, $(0, 0, z_{\text{graz}, \eta}) \in \Sigma_{\text{graz}}$.

We assume that the codimension-two scenarios occur at $\eta = 0$, and that the above quantities, τ , etc, are now evaluated at $\eta = 0$. For all $p \geq 1$, let

$$\xi_p = \frac{\partial^2 P_{\text{global}, 1}^p}{\partial z^2} \Big|_{(x, z; \mu, \eta) = (0, z_{\text{graz}, 0}; 0, 0)}, \quad (2.19)$$

where $P_{\text{global}, 1}^p$ is the first component of the p^{th} iterate of P_{global} . For $p = 1$, let

$$s_1^\pm = (1 \mp a_{22})(a_{11}\phi^2 \mp 1) + \frac{\alpha^2\omega^2\xi_1}{(1 - a_{22})\gamma}. \quad (2.20)$$

Also let $a'_{12} = \frac{da_{12}}{d\eta}|_{\eta=0}$, and

$$c_{\text{SN},1} = \frac{(\alpha\omega a'_{12})^2}{2\beta\gamma s_1^+}, \quad c_{\text{PD},1} = \frac{s_1^+}{s_1^-} \left(2 - \frac{s_1^+}{s_1^-} \right) c_{\text{SN},1}. \quad (2.21)$$

Theorem 2.4 (resonant grazing, $p = 1$). *Consider an impacting hybrid system (2.3)–(2.5) where F and R are C^k ($k \geq 5$). Suppose Assumption 2.2 holds, $(\tau, \delta) \in \mathcal{T}$, $\alpha > 0$, $\beta \neq 0$, $a_{12} = 0$, $a'_{12} \neq 0$, and $s_1^\pm \neq 0$. Then there exist local C^{k-2} functions*

$$g_{\text{SN},1}(\eta) = c_{\text{SN},1}\eta^2 + \mathcal{O}(\eta^3), \quad (2.22)$$

$$g_{\text{PD},1}(\eta) = c_{\text{PD},1}\eta^2 + \mathcal{O}(\eta^3), \quad (2.23)$$

such that a one-loop MPS undergoes a saddle-node bifurcation when $\mu = g_{\text{SN},1}(\eta)$, with $\text{sgn}(\eta) = \text{sgn}(a'_{12}s_1^+)$, and has a stability multiplier of -1 when $\mu = g_{\text{PD},1}(\eta)$, with $\text{sgn}(\eta) = \text{sgn}(a'_{12}s_1^-)$.

For all $p \geq 2$, let

$$s_p^\pm = \left(1 \pm \delta^{\frac{p}{2}} \right) \left(-\delta^{\frac{p}{2}}\phi^2 \mp 1 \right) + \frac{\alpha^2\omega^2\xi_p}{(1 + \delta^{\frac{p}{2}})\gamma}. \quad (2.24)$$

Also let $\kappa'_p = \frac{d\kappa_p}{d\eta}|_{\eta=0}$, and

$$c_{\text{SN},p} = \left(\frac{pa_{12}\alpha\omega\delta^{\frac{p}{2}-1}\kappa'_p}{2\sin^2(\frac{\pi}{p})(1 + \delta^{\frac{p}{2}})} \right)^2 \frac{\delta - \tau + 1}{2\beta\gamma s_p^+}, \quad c_{\text{PD},p} = \frac{s_p^+}{s_p^-} \left(2 - \frac{s_p^+}{s_p^-} \right) c_{\text{SN},p}. \quad (2.25)$$

Theorem 2.5 (resonant grazing, $p \geq 2$). *Consider an impacting hybrid system (2.3)–(2.5) where F and R are C^k ($k \geq 5$), and let $p \geq 2$. Suppose Assumption 2.2 holds, $(\tau, \delta) \in \mathcal{T}$, $a_{12}\alpha > 0$, $\beta \neq 0$, $\kappa_p = 0$, $\kappa'_p \neq 0$, and $s_p^\pm \neq 0$. Then there exist local C^{k-2} functions*

$$g_{\text{SN},p}(\eta) = c_{\text{SN},p}\eta^2 + \mathcal{O}(\eta^3), \quad (2.26)$$

$$g_{\text{PD},p}(\eta) = c_{\text{PD},p}\eta^2 + \mathcal{O}(\eta^3), \quad (2.27)$$

such that a p -loop MPS undergoes a saddle-node bifurcation when $\mu = g_{\text{SN},p}(\eta)$, with $\text{sgn}(\eta) = \text{sgn}(\kappa'_p s_p^+)$, and has a stability multiplier of -1 when $\mu = g_{\text{PD},p}(\eta)$, with $\text{sgn}(\eta) = \text{sgn}(\kappa'_p s_p^-)$.

Fig. 5 provides a sketch of a typical two-parameter bifurcation diagram showing the curves predicted by Theorems 2.4 and 2.5. In generic situations, $\mu = g_{\text{PD},p}(\eta)$ is a curve of period-doubling bifurcations of the p -loop MPS. We have not computed the quadratic and cubic terms necessary to evaluate the non-degeneracy condition that ensures period-doubling bifurcations do occur on this curve, as this appears to be extremely challenging to achieve in a general setting. For the curve $\mu = g_{\text{SN},p}(\eta)$, we compute in §5 the key quadratic term that shows saddle-node bifurcation occur on this curve.

Remark 2.1. In Theorem 2.4, $a_{12} = 0$, thus $\beta = (1 - a_{22})b_1$. Hence in this case the assumption $\beta \neq 0$ implies $a_{22} \neq 1$ and $b_1 \neq 0$.

3 A harmonically forced linear oscillator

In this section we apply the above theory to the forced linear oscillator depicted in Fig. 6.

3.1 Equations of motion and grazing of the non-impacting periodic solution

For the motion of the block in Fig. 6, we use the non-dimensionalised equation

$$\ddot{x} + 2\zeta\dot{x} + x + 1 = \mathcal{A} \cos(\omega t), \quad (3.1)$$

where ζ is the damping ratio, \mathcal{A} is the forcing amplitude, and ω is the forcing frequency. We assume impacts of the block with the wall occur instantaneously with coefficient of restitution ϵ :

$$y \mapsto -\epsilon y, \quad \text{when } x = 0 \text{ with } y > 0. \quad (3.2)$$

The equilibrium position of the oscillator is $x = -1$. With $0 < \zeta < 1$, the oscillator is under-damped and the eigenvalues associated with the equilibrium are $-\zeta \pm i\omega_1$, where

$$\omega_1 = \sqrt{1 - \zeta^2}$$

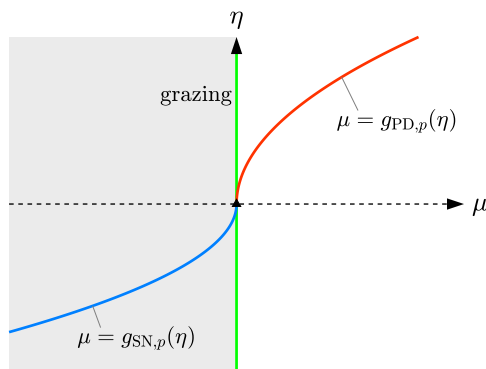


Figure 5: A sketch of the bifurcation curves described by Theorems 2.4 and 2.5 in the case $c_{SN,p} < 0$, $c_{PD,p} > 0$, and $\beta > 0$. Here a stable non-impacting periodic solution exists for $\mu < 0$.

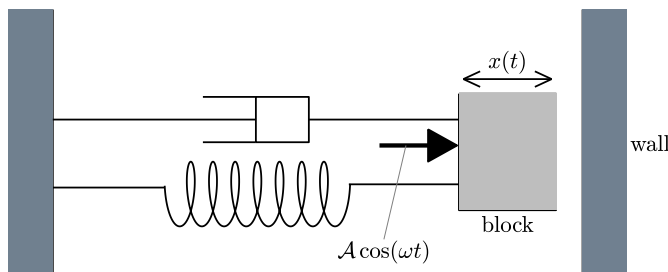


Figure 6: A sketch of the impact oscillator modelled by (3.1)–(3.2).

is the damped natural frequency. Given $(x, \dot{x}) = (x_0, y_0)$ at time t_0 , the solution to (3.1) is

$$\begin{aligned} \phi(t; x_0, y_0, t_0; \mathcal{A}) = & e^{-\zeta(t-t_0)} \left(\left(\cos(\omega_1(t-t_0)) + \frac{\zeta}{\omega_1} \sin(\omega_1(t-t_0)) \right) (x_0 - \phi_p(t_0; \mathcal{A})) \right. \\ & \left. + \frac{1}{\omega_1} \sin(\omega_1(t-t_0)) (y_0 - \dot{\phi}_p(t_0; \mathcal{A})) \right) + \phi_p(t; \mathcal{A}), \end{aligned} \quad (3.3)$$

where

$$\phi_p(t; \mathcal{A}) = -1 + \frac{\mathcal{A}}{(1-\omega^2)^2 + 4\zeta^2\omega^2} \left((1-\omega^2) \cos(\omega t) + 2\zeta\omega \sin(\omega t) \right). \quad (3.4)$$

As $t \rightarrow \infty$, the solution converges to $\phi_p(t)$, which is an asymptotically stable period- $\frac{2\pi}{\omega}$ non-impacting solution. This periodic solution grazes the wall when its maximum x -value is zero. It is a simple exercise to show from (3.4) that this occurs when $\mathcal{A} = \mathcal{A}_{\text{graz}}(\omega)$, where

$$\mathcal{A}_{\text{graz}}(\omega) = \sqrt{(1-\omega^2)^2 + 4\zeta^2\omega^2}. \quad (3.5)$$

At grazing, the phase $z = \omega t \bmod 2\pi$ is $z = z_{\text{graz}}$, where

$$\sin(z_{\text{graz}}) = \frac{2\zeta\omega}{\mathcal{A}_{\text{graz}}(\omega)}, \quad \cos(z_{\text{graz}}) = \frac{1-\omega^2}{\mathcal{A}_{\text{graz}}(\omega)}. \quad (3.6)$$

3.2 Numerical bifurcation analysis

Motivated by physical experiments reported in [29, 34], we fix $\zeta = 0.02$ and $\epsilon = 0.9$, corresponding to relatively low damping and energy loss at impacts. Fig. 7 shows a numerically computed two-parameter bifurcation diagram for the system at these parameter values. The light green curve is the grazing bifurcation $\mathcal{A} = \mathcal{A}_{\text{graz}}(\omega)$. To the left of this curve (light grey) the non-impacting solution $\phi_p(t)$ is an asymptotically stable solution of the full system.

The other shaded regions (dark grey) are where the system has an asymptotically stable p -loop MPS for $p = 1, 2, 3$. Each of these regions is bounded by three curves: a curve PD where the MPS loses stability in a period-doubling bifurcation, a curve SN where the MPS collides and annihilates with an unstable MPS of the same period, and a curve GZ where the MPS is destroyed in a grazing bifurcation. These curves were continued numerically using the approach of [28] that employs a root-finding method to locate zeros of the VIVID function, see §4.3.

3.3 Parameter values associated with grazing

The saddle-node and period-doubling bifurcation curves arise from points of resonance on the grazing curve $\mathcal{A} = \mathcal{A}_{\text{graz}}(\omega)$. To compute these points, we first observe that the impact oscillator model takes the general form (2.3)–(2.5) with

$$F(x, \dot{x}, t) = -2\zeta\dot{x} - x - 1 + \mathcal{A} \cos(\omega t), \quad \Phi(y, z) = \epsilon, \quad \Psi(y, z) = 0.$$

By evaluating (2.18), we obtain

$$\phi = \epsilon, \quad \psi = 0, \quad \gamma = \omega^2, \quad (3.7)$$

and thus

$$\alpha = 1 + \epsilon, \quad (3.8)$$

by (2.17). To apply the theory of §2, we treat $\mu = \mathcal{A} - \mathcal{A}_{\text{graz}}(\omega)$ as the primary bifurcation parameter.

Proposition 3.1. *The first derivatives of P_{global} at grazing, (2.7) and (2.8), are given by*

$$A = e^{-\frac{2\pi\zeta}{\omega}} \begin{bmatrix} \cos\left(\frac{2\pi\omega_1}{\omega}\right) + \frac{\zeta}{\omega_1} \sin\left(\frac{2\pi\omega_1}{\omega}\right) & \frac{\omega}{\omega_1} \sin\left(\frac{2\pi\omega_1}{\omega}\right) \\ \frac{-1}{\omega_1\omega} \sin\left(\frac{2\pi\omega_1}{\omega}\right) & \cos\left(\frac{2\pi\omega_1}{\omega}\right) - \frac{\zeta}{\omega_1} \sin\left(\frac{2\pi\omega_1}{\omega}\right) \end{bmatrix}, \quad (3.9)$$

$$b = \frac{1}{\mathcal{A}_{\text{graz}}(\omega)} \begin{bmatrix} 1 - a_{11} \\ -a_{21} \end{bmatrix}, \quad (3.10)$$

where again we write a_{ij} for the (i, j) -entry of A .

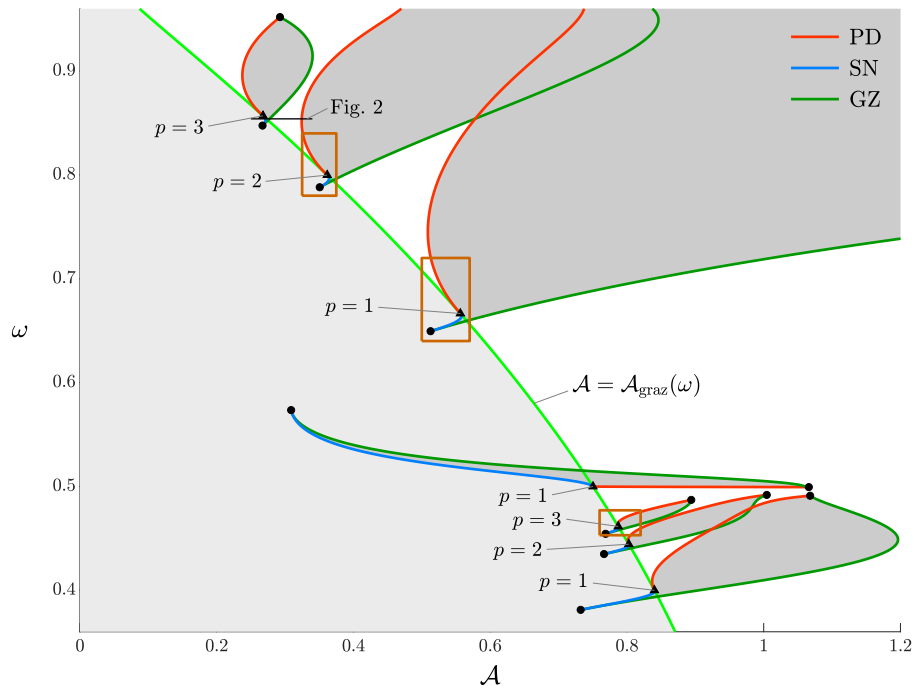


Figure 7: A two-parameter bifurcation diagram of the impact oscillator model (3.1)–(3.2) with $\zeta = 0.02$ and $\epsilon = 0.9$. The parameters on the axes are the forcing amplitude \mathcal{A} , and the forcing frequency ω . The curve $\mathcal{A} = \mathcal{A}_{\text{graz}}(\omega)$ is the grazing bifurcation (3.5) of the non-impacting periodic solution. The red, blue, and dark green curves are period-doubling, saddle-node, and grazing bifurcations of p -loop MPSs for $p = 1, 2, 3$. These curves meet at resonant grazing bifurcations (black triangles), and other codimension-two points (black circles). Magnified views of the diagram over the orange rectangles are shown in Fig. 8. The line segment at $\omega = 0.854$ corresponds to the one-parameter bifurcation diagram shown in Fig. 2.

The formulas (3.9) and (3.10) are derived in Appendix B by expanding the explicit solution (3.3) to first order. The trace and determinant of (3.9) are

$$\tau = 2e^{-\frac{2\pi\zeta}{\omega}} \cos\left(\frac{2\pi\omega_1}{\omega}\right), \quad \delta = e^{-\frac{4\pi\zeta}{\omega}}, \quad (3.11)$$

and by evaluating (2.12) we obtain

$$\beta = \frac{\delta - \tau + 1}{\mathcal{A}_{\text{graz}}(\omega)}.$$

3.4 Points of resonance

For $p = 1$, the codimension-two scenario occurs when $a_{12} = 0$. By (3.9), $a_{12} = 0$ if and only if

$$\frac{\omega_1}{\omega} = \frac{n}{2}, \quad (3.12)$$

for some $n \in \mathbb{Z}$. In Fig. 7, the points on $\mathcal{A} = \mathcal{A}_{\text{graz}}(\omega)$ labelled $p = 1$ correspond to (3.12) with $n = 3, 4, 5$: specifically, $\omega = \frac{2\omega_1}{3} \approx 0.6665$, $\omega = \frac{2\omega_1}{4} \approx 0.4999$, and $\omega = \frac{2\omega_1}{5} \approx 0.3999$.

For $p \geq 2$, the codimension-two scenario occurs when $\tau = g_p(\delta)$, where $g_p(\delta) = 2\sqrt{\delta} \cos\left(\frac{\pi}{p}\right)$. By (3.11), $\tau = g_p(\delta)$ if and only if

$$\frac{\omega_1}{\omega} = n \pm \frac{1}{2p}, \quad (3.13)$$

for some $n \in \mathbb{Z}$. In Fig. 7, the points on $\mathcal{A} = \mathcal{A}_{\text{graz}}(\omega)$ labelled $p = 2, 3$ correspond to $\frac{\omega_1}{\omega} = n + \frac{1}{2p}$ with $n = 1, 2$. Points with $\frac{\omega_1}{\omega} = n - \frac{1}{2p}$ do not produce the codimension-two phenomenon because in this case the MPSs are virtual. This can be explained as follows. By substituting (3.13) into the (1, 2) entry of (3.9), we obtain

$$a_{12} = \frac{\pm e^{-\frac{2\pi\zeta}{\omega}}}{n \pm \frac{1}{2p}} \sin\left(\frac{\pi}{p}\right).$$

By (3.8), if a positive sign is used in (3.13) then $a_{12}\alpha > 0$, while if a negative sign is used in (3.13) then $a_{12}\alpha < 0$. Theorem 2.5 requires $a_{12}\alpha > 0$; if $a_{12}\alpha < 0$ then the MPSs are virtual as can be inferred from calculations performed in §4.4.

Pavlovskaja *et al.* [29] provide experimentally computed bifurcation diagrams of a physical dynamic shaker. They use ω as the primary bifurcation parameter and obtain grazing at $\omega \approx 0.8$. This is near the $p = 2$ resonance point $\frac{\omega_1}{\omega} = n + \frac{1}{2p}$ with $n = 1$, specifically $\omega = \frac{4\omega_1}{5} \approx 0.7998$, at which a stable two-loop MPS is generated. This explains why their bifurcation diagram [29, Figure 3] shows that a stable two-loop MPS is the dominant attractor just beyond the grazing bifurcation.

3.5 Quadratic approximations to the saddle-node and period-doubling bifurcation curves

To apply Theorems 2.4 and 2.5, we use ω as the secondary parameter. Specifically, we let $\eta = \omega - \omega^*$, where we write ω^* for the value of ω at the resonant grazing bifurcation.

By further using the flow (3.3), we obtain the following formulas for a'_{12} , κ'_p , s_p^\pm and the quadratic coefficients $c_{\text{SN},p}$ and $c_{\text{PD},p}$. These formulas are derived in Appendix B. For brevity we write

$$E_p = e^{-\frac{2\pi p \zeta}{\omega}}, \quad (3.14)$$

and notice from (3.11) that $E_p = \delta^{\frac{p}{2}}$.

Proposition 3.2 (resonant grazing, $p = 1$). *Consider the impact oscillator (3.1)–(3.2) with $\mathcal{A} = \mathcal{A}_{\text{graz}}(\omega)$ and $\frac{\omega_1}{\omega} = \frac{n}{2}$, where $n \geq 1$ is an integer. If n is odd, then*

$$\begin{aligned} a'_{12} &= \frac{2\pi E_1}{\omega}, \\ s_1^+ &= -(1 - \epsilon E_1)^2, \\ s_1^- &= (1 + \epsilon E_1)^2, \\ c_{\text{SN},1} &= -\frac{2\pi^2 A_{\text{graz}}}{\omega^2} \left(\frac{(1 + \epsilon)E_1}{(1 - \epsilon E_1)(1 + E_1)} \right)^2, \\ c_{\text{PD},1} &= -\frac{(1 - \epsilon E_1)^2 ((1 + \epsilon E_1)^2 + 2(1 + \epsilon^2 E_1^2))}{(1 + \epsilon E_1)^4} c_{\text{SN},1}, \end{aligned} \quad (3.15)$$

while if n is even, then

$$\begin{aligned} a'_{12} &= -\frac{2\pi E_1}{\omega}, \\ s_1^+ &= -(1 + \epsilon E_1)^2, \\ s_1^- &= (1 - \epsilon E_1)^2, \\ c_{\text{SN},1} &= -\frac{2\pi^2 A_{\text{graz}}}{\omega^2} \left(\frac{(1 + \epsilon)E_1}{(1 + \epsilon E_1)(1 - E_1)} \right)^2, \\ c_{\text{PD},1} &= -\frac{(1 + \epsilon E_1)^2 ((1 - \epsilon E_1)^2 + 2(1 + \epsilon^2 E_1^2))}{(1 - \epsilon E_1)^4} c_{\text{SN},1}. \end{aligned} \quad (3.16)$$

Proposition 3.3 (resonant grazing, $p \geq 2$). *For the impact oscillator (3.1)–(3.2) with $\mathcal{A} = \mathcal{A}_{\text{graz}}(\omega)$ and $\frac{\omega_1}{\omega} = n + \frac{1}{2p}$, where $n \geq 1$ and $p \geq 2$ are integers,*

$$\begin{aligned} \kappa'_p &= \frac{4\pi\omega_1}{\omega^2} e^{-\frac{2\pi\zeta}{\omega}} \sin\left(\frac{\pi}{p}\right), \\ s_1^+ &= -(1 - \epsilon E_p)^2, \\ s_1^- &= (1 + \epsilon E_p)^2, \\ c_{\text{SN},p} &= -\frac{2\pi^2 p^2 A_{\text{graz}}}{\omega^2} \left(\frac{(1 + \epsilon)E_p}{(1 - \epsilon E_p)(1 + E_p)} \right)^2, \\ c_{\text{PD},p} &= -\frac{(1 - \epsilon E_p)^2 ((1 + \epsilon E_p)^2 + 2(1 + \epsilon^2 E_p^2))}{(1 + \epsilon E_p)^4} c_{\text{SN},p}. \end{aligned} \quad (3.17)$$

To illustrate Propositions 3.2 and 3.3, Fig. 8 shows magnifications of Fig. 7 about three points of resonance. In these magnifications we have overlaid the quadratic approximations $\mu = c_{\text{SN},p}\eta^2$ and $\mu = c_{\text{PD},p}\eta^2$ (dashed). This was achieved by evaluating (3.15) and (3.17), and inverting the coordinate change $(\mu, \eta) = (\mathcal{A} - \mathcal{A}_{\text{graz}}(\omega), \omega - \omega^*)$. As expected, the quadratic approximations provide a good fit to the bifurcation curves as they emanate from the codimension-two points.

Propositions 3.2 and 3.3 show that if $\epsilon \neq \frac{1}{E_p}$, then $c_{\text{SN},p} < 0$ and $c_{\text{PD},p} > 0$ for all $p \geq 1$. In this case the saddle-node and period-doubling bifurcation curves exist on different sides of $\mathcal{A} = \mathcal{A}_{\text{graz}}$, as in Fig. 7. Furthermore, in this case s_p^+ and s_p^- have different signs, so by Theorems 2.3 and 2.5 the saddle-node and period-doubling bifurcation curves grow in opposite directions out of the resonant grazing point, as seen for all points of resonance indicated in Fig. 7.

4 Calculations for generic grazing bifurcations

In this section we prove Theorems 2.2 and 2.3. First in §4.1 we compute the components of the discontinuity map, then in §4.2 characterise the p^{th} iterate of the global map to first order. In §4.3 we define the VIVID function and compute its derivatives, then in §4.4 combine the computations to verify Theorems 2.2 and 2.3. Throughout this section we ignore the second parameter η , and write ω in place of $\omega(0)$.

4.1 The discontinuity map

We first introduce some additional notation. Suppose an orbit of (2.3)–(2.5) reaches the impacting surface at a point $(0, y_{\text{imp}}, z_{\text{imp}})$ on the incoming set, i.e. $y_{\text{imp}} > 0$, see Fig. 9. This

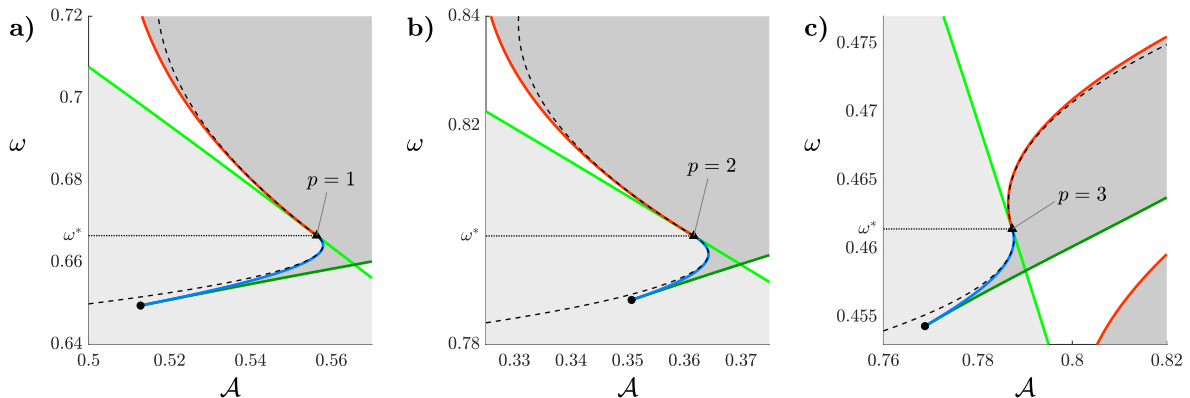


Figure 8: Magnifications of Fig. 7; the dashed curves show $\mu = c_{\text{SN},p}\eta^2$ and $\mu = c_{\text{PD},p}\eta^2$ where $c_{\text{SN},p}$ and $c_{\text{PD},p}$ are given by Propositions 3.2 and 3.3. To four significant figures, $c_{\text{SN},1} = -282.4$ and $c_{\text{PD},1} = 12.15$ for the left plot, $c_{\text{SN},2} = -244.5$ and $c_{\text{PD},2} = 21.35$ for the middle plot, and $c_{\text{SN},3} = -613.4$ and $c_{\text{PD},3} = 249.1$ for the right plot.

orbit subsequently departs the impacting surface from the point $(0, y_{\text{rec}}, z_{\text{rec}})$, where

$$(y_{\text{rec}}, z_{\text{rec}}) = R(y_{\text{imp}}, z_{\text{imp}}; \mu), \quad (4.1)$$

belongs to the outgoing set, i.e. $y_{\text{rec}} < 0$.

Now consider a smooth extension of F into $x > 0$. We evolve under the ODEs (2.3) into $x > 0$ from the impacting point forwards in time until reaching Π at a point $(\hat{x}, 0, \hat{z})$, and from the recoil point backwards in time until reaching Π at a point $(x^{(0)}, 0, z^{(0)})$. These points are *virtual* because they do not belong to orbits of the full system (2.3)–(2.5).

Let $(x', z') = P_{\text{virt}}(y, z; \mu)$ be the map that takes points from Σ to Π following (2.3), so

$$(\hat{x}, \hat{z}) = P_{\text{virt}}(y_{\text{imp}}, z_{\text{imp}}; \mu), \quad (x^{(0)}, z^{(0)}) = P_{\text{virt}}(y_{\text{rec}}, z_{\text{rec}}; \mu). \quad (4.2)$$

The map is evaluated by evolving forwards in time from Σ if $y > 0$, and backwards in time from Σ if $y < 0$ (if $y = 0$ the evolution time is zero and $(x', z') = (0, z)$). This stipulation on the direction of time ensures that the evolution time is small when the value of y is small. By considering smooth extensions of Φ and Ψ into $y < 0$, the above points are well defined for small $y_{\text{imp}} < 0$.

If F is C^k , then P_{virt} is C^k at any $(y_{\text{imp}}, z_{\text{imp}}; \mu)$ for which the associated orbit hits Π transversally (this is a consequence of the implicit function theorem [35]). With Assumption 2.1, transversality is satisfied at grazing, thus P_{virt} is C^k in a neighbourhood of $(0, z_{\text{graz}}; 0)$.

Given $(y_{\text{imp}}, z_{\text{imp}}; \mu)$ near $(0, z_{\text{graz}}; 0)$, the following result provides asymptotic formulas for (\hat{x}, \hat{z}) and $(x^{(0)}, z^{(0)})$ which involve the constants defined in (2.18). A derivation is provided below. Similar calculations can be found in [26, 36].

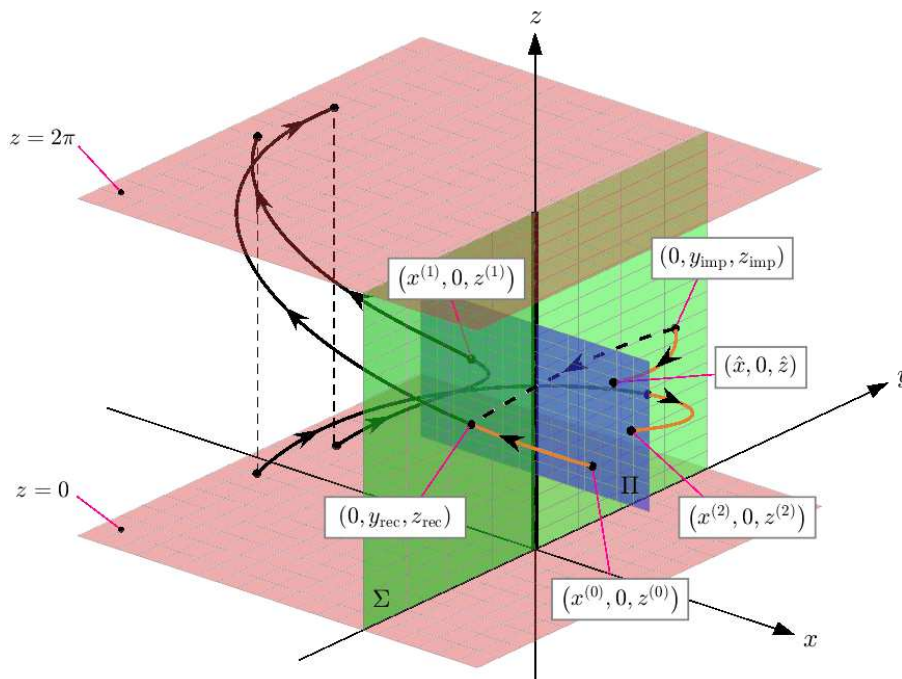


Figure 9: A sketch indicating points defined in the text where an orbit intersects Σ and Π .

Lemma 4.1. *We have*

$$\begin{aligned}\hat{x} &= \frac{y_{\text{imp}}^2}{2\gamma} + \mathcal{O}((|y_{\text{imp}}| + |z_{\text{imp}} - z_{\text{graz}}| + |\mu|)^3), \\ \hat{z} &= \frac{\omega y_{\text{imp}}}{\gamma} + z_{\text{imp}} + \mathcal{O}((|y_{\text{imp}}| + |z_{\text{imp}} - z_{\text{graz}}| + |\mu|)^2),\end{aligned}\tag{4.3}$$

and

$$\begin{aligned}x^{(0)} &= \frac{\phi^2 y_{\text{imp}}^2}{2\gamma} + \mathcal{O}((|y_{\text{imp}}| + |z_{\text{imp}} - z_{\text{graz}}| + |\mu|)^3), \\ z^{(0)} &= \frac{\omega(1-\alpha)}{\gamma} y_{\text{imp}} + z_{\text{imp}} + \mathcal{O}((|y_{\text{imp}}| + |z_{\text{imp}} - z_{\text{graz}}| + |\mu|)^2).\end{aligned}\tag{4.4}$$

Proof. The ODEs (2.3) can be written as

$$\begin{bmatrix} \dot{x} \\ \dot{y} \\ \dot{z} \end{bmatrix} = \begin{bmatrix} y \\ -\gamma + \mathcal{O}(|x| + |y| + |z - z_{\text{graz}}| + |\mu|) \\ \omega + \mathcal{O}(\mu) \end{bmatrix}.$$

Thus the orbit of (2.3) through $(x, y, z) = (0, y_{\text{imp}}, z_{\text{imp}})$ is given by

$$\begin{aligned}x(t) &= y_{\text{imp}}t - \frac{\gamma t^2}{2} + \mathcal{O}((|y_{\text{imp}}| + |z_{\text{imp}} - z_{\text{graz}}| + |\mu| + |t|)^3), \\ y(t) &= y_{\text{imp}} - \gamma t + \mathcal{O}((|y_{\text{imp}}| + |z_{\text{imp}} - z_{\text{graz}}| + |\mu| + |t|)^2), \\ z(t) &= z_{\text{imp}} + \omega t + \mathcal{O}((|\mu| + |t|)^2).\end{aligned}$$

Since $\gamma \neq 0$, we can solve $y(T) = 0$ for the evolution time T , resulting in

$$T(y_{\text{imp}}, z_{\text{imp}}; \mu) = \frac{y_{\text{imp}}}{\gamma} + \mathcal{O}((|y_{\text{imp}}| + |z_{\text{imp}} - z_{\text{graz}}| + |\mu|)^2),$$

and by substituting this into $x(t)$ and $z(t)$ we obtain (4.3). The reset law (2.4) can be written as

$$\begin{bmatrix} y \\ z \end{bmatrix} \mapsto \begin{bmatrix} -y(\phi + \mathcal{O}(|y| + |z - z_{\text{graz}}| + |\mu|)) \\ z + y(\psi + \mathcal{O}(|y| + |z - z_{\text{graz}}| + |\mu|)) \end{bmatrix},$$

thus

$$\begin{aligned}y_{\text{rec}} &= -\phi y_{\text{imp}} + \mathcal{O}((|y_{\text{imp}}| + |z_{\text{imp}} - z_{\text{graz}}| + |\mu|)^2), \\ z_{\text{rec}} &= \psi y_{\text{imp}} + z_{\text{imp}} + \mathcal{O}((|y_{\text{imp}}| + |z_{\text{imp}} - z_{\text{graz}}| + |\mu|)^2).\end{aligned}$$

By using these in place of y_{imp} and z_{imp} in (4.3), and inserting the formula (2.17) for α , we obtain (4.4). \square

For $x > 0$, the inverse P_{virt}^{-1} has two values: one on the incoming set $y > 0$, and one on the outgoing set $y < 0$. Throughout this paper we always take the value on the incoming set. Then

$$P_{\text{disc}} = P_{\text{virt}} \circ R \circ P_{\text{virt}}^{-1}, \quad (4.5)$$

is well-defined, and is the *discontinuity map* that takes (\hat{x}, \hat{z}) to $(x^{(0)}, z^{(0)})$. By inverting (4.3) and substituting the result into (4.4), we obtain

$$\begin{aligned} x^{(0)} &= \phi_0^2 \hat{x} + \dots, \\ z^{(0)} &= -\frac{\alpha\omega\sqrt{2}}{\sqrt{\gamma}} \sqrt{\hat{x}} + \hat{z} + \dots, \end{aligned} \quad (4.6)$$

to leading order. This shows that P_{disc} contains a square-root term whose sign is controlled by the sign of α .

4.2 Iterates of the global map.

Define

$$S_j = \sum_{k=1}^j \lambda_1^{j-k} \lambda_2^{k-1}, \quad T_p = \sum_{j=1}^{p-1} S_j. \quad (4.7)$$

where λ_1 and λ_2 are the eigenvalues of A , see (2.13). By (2.16), $H_p(\tau, \delta) = \sum_{j=1}^{p-1} \frac{S_j}{\delta^{j-1}}$ (since $\lambda_1 \lambda_2 = \delta$). Moreover,

$$H_p(\tau, \delta) = \frac{S_{p-1} T_p - S_p T_{p-1}}{\delta^{p-2}}, \quad (4.8)$$

for all $p \geq 1$. By composing the first-order expression (2.6) of P_{global} with itself p times, we obtain

$$P_{\text{global}}^p(x, z; \mu) = \begin{bmatrix} 0 \\ z_{\text{graz}} \end{bmatrix} + A^p \begin{bmatrix} x \\ z - z_{\text{graz}} \end{bmatrix} + \begin{bmatrix} b_{1p} \\ b_{2p} \end{bmatrix} \mu + \mathcal{O}((|x| + |z - z_{\text{graz}}| + |\mu|)^2), \quad (4.9)$$

where

$$A^p = S_{p+1} I + S_p \begin{bmatrix} -a_{22} & a_{12} \\ a_{21} & -a_{11} \end{bmatrix}, \quad (4.10)$$

$$\begin{bmatrix} b_{1p} \\ b_{2p} \end{bmatrix} = S_p \begin{bmatrix} b_1 \\ b_2 \end{bmatrix} + T_p \begin{bmatrix} \beta \\ a_{21} b_1 + (1 - a_{11}) b_2 \end{bmatrix}. \quad (4.11)$$

The formulas (4.10) and (4.11) were derived via Sylvester's formula [37], and can be verified by induction on p . The following result is proved in Appendix A.

Lemma 4.2. *Let $p \geq 2$ and $(\tau, \delta) \in \mathcal{T}$.*

- (a) *If $\tau > h_p(\delta)$, then $\text{sgn}(S_p) = \text{sgn}(\tau - g_p(\delta))$.*
- (b) *If $\tau = g_p(\delta)$, then $S_{p+1} = -\delta^{\frac{p}{2}}$ and $T_p = \frac{1+\delta^{\frac{p}{2}}}{\delta^{-\tau+1}}$.*
- (c) *If $\tau \geq g_{\frac{p}{2}}(\delta)$, then $T_p > 0$.*

4.3 The VIVID function

Given $p \geq 1$, for all $j = 1, 2, \dots, p$ let

$$(x^{(j)}, z^{(j)}) = P_{\text{global}}(x^{(j-1)}, z^{(j-1)}; \mu), \quad (4.12)$$

as indicated in Fig. 9 for $p = 2$. These points correspond to a p -loop MPS if $(x^{(p)}, z^{(p)}) = (\hat{x}, \hat{z})$. In this case (\hat{x}, \hat{z}) is a fixed point of $P_{\text{global}}^p \circ P_{\text{disc}}$, so can be found by solving for fixed points of this map. However, we require smoothness, so instead search for zeros of the VIVID function

$$V(y_{\text{imp}}, z_{\text{imp}}; \mu) = (x^{(p)}, z^{(p)}) - (\hat{x}, \hat{z}). \quad (4.13)$$

Notice $V = P_{\text{global}}^p \circ P_{\text{virt}} \circ R - P_{\text{virt}}$ is comprised of C^k functions, so is C^k and well-defined in a neighbourhood of the grazing bifurcation.

By Assumption 2.1, $V(0, z_{\text{graz}}; 0) = (0, 0)$. Write $V(y, z; \mu) = (V_1, V_2)$ and define

$$J = \left[\begin{array}{cc} \frac{\partial V_1}{\partial y} & \frac{\partial V_1}{\partial z} \\ \frac{\partial V_2}{\partial y} & \frac{\partial V_2}{\partial z} \end{array} \right] \Big|_{(y,z;\mu)=(0,z_{\text{graz}};0)}, \quad K = \left[\begin{array}{cc} \frac{\partial V_1}{\partial z} & \frac{\partial V_1}{\partial \mu} \\ \frac{\partial V_2}{\partial z} & \frac{\partial V_2}{\partial \mu} \end{array} \right] \Big|_{(y,z;\mu)=(0,z_{\text{graz}};0)}. \quad (4.14)$$

To find zeros of V , we use the implicit function theorem. This requires the invertibility of J or K .

Lemma 4.3. *For all $p \geq 1$, the determinants of (4.14) are given by*

$$\det(J) = \frac{\alpha a_{12} \omega S_p}{\gamma}, \quad \det(K) = (1 - S_{p+1} + a_{11} S_p) b_{1p} + a_{12} S_p b_{2p}. \quad (4.15)$$

Moreover, if $\tau \neq \delta + 1$ then

$$\det(K) = \frac{(1 - \lambda_1^p)(1 - \lambda_2^p)\beta}{(1 - \lambda_1)(1 - \lambda_2)}. \quad (4.16)$$

Proof. By combining (4.3), (4.4), (4.9), and (4.10) we obtain

$$\begin{aligned} V_1 &= \frac{a_{12} \omega (1 - \alpha) S_p}{\gamma} y_{\text{imp}} + a_{12} S_p (z_{\text{imp}} - z_{\text{graz}}) + b_{1p} \mu \\ &\quad + \mathcal{O}((|y_{\text{imp}}| + |z_{\text{imp}} - z_{\text{graz}}| + |\mu|)^2), \end{aligned} \quad (4.17)$$

$$\begin{aligned} V_2 &= \frac{\omega}{\gamma} ((1 - \alpha)(S_{p+1} - a_{11} S_p) - 1) y_{\text{imp}} + (S_{p+1} - a_{11} S_p - 1)(z_{\text{imp}} - z_{\text{graz}}) + b_{2p} \mu \\ &\quad + \mathcal{O}((|y_{\text{imp}}| + |z_{\text{imp}} - z_{\text{graz}}| + |\mu|)^2), \end{aligned} \quad (4.18)$$

using also the formula (2.17) for α . Thus we read off

$$J = \left[\begin{array}{cc} \frac{a_{12} \omega (1 - \alpha) S_p}{\gamma} & a_{12} S_p \\ \frac{\omega}{\gamma} ((1 - \alpha)(S_{p+1} - a_{11} S_p) - 1) & S_{p+1} - a_{11} S_p - 1 \end{array} \right], \quad K = \left[\begin{array}{cc} a_{12} S_p & b_{1p} \\ S_{p+1} - a_{11} S_p - 1 & b_{2p} \end{array} \right],$$

and by evaluating the determinants of these matrices we obtain (4.15). If $\tau \neq \delta + 1$, then $S_p = \frac{\lambda_1^p - \lambda_2^p}{\lambda_1 - \lambda_2}$, see (A.10), and by combining this with (4.11) we obtain (4.16) after algebraic simplification. \square

4.4 Main arguments for generic grazing bifurcations

Proof of Theorem 2.2. Putting $p = 1$ into (4.15) gives $\det(J) = \frac{\alpha a_{12} \omega}{\gamma} \neq 0$, because $S_1 = 1$. Also $\tau \neq \delta + 1$, because $(\tau, \delta) \in \mathcal{T}$, so $\det(K) = \beta \neq 0$ by (4.16). We now use (4.17) and (4.18) to solve $V(y; z; \mu) = (0, 0)$ for y and z in terms μ . Since V is C^3 and $\det(J) \neq 0$, by the implicit function theorem there exists a unique C^3 solution

$$y^*(\mu) = \frac{\gamma \beta}{\alpha a_{12} \omega} \mu + \mathcal{O}(\mu^2), \quad (4.19)$$

$$z^*(\mu) = z_{\text{graz}} + \frac{1}{\alpha a_{12}} ((a_{22}(1 - \alpha) - 1)b_1 - a_{12}(1 - \alpha)b_2) \mu + \mathcal{O}(\mu^2), \quad (4.20)$$

for small $\mu \in \mathbb{R}$. This corresponds to a one-loop MPS if $y^*(\mu) > 0$ and μ is sufficiently small. By assumption $\alpha > 0$, $\omega > 0$, and $\gamma > 0$. Thus if $a_{12}\beta > 0$, then $y^*(\mu) > 0$ for small $\mu > 0$, while if $a_{12}\beta < 0$, then $y^*(\mu) > 0$ for small $\mu < 0$. \square

Proof of Theorem 2.3. The proof is completed in three steps. In Step 1 we compute a zero of the VIVID function corresponding to a p -loop MPS, then map it under R , P_{virt} , and P_{global} to identify all points where the p -loop MPS intersects the Poincaré section Π . In Step 2 we remove higher-order terms, so that in Step 3 admissibility can be characterised through brute-force algebraic computations and the geometric properties of a linear map.

Step 1 — Calculate points.

Suppose $\kappa_p \neq 0$, i.e. $\tau \neq g_p(\delta)$. By Lemma 4.2(a), $\text{sgn}(S_p) = \text{sgn}(\kappa_p)$, and so $\det(J) \neq 0$ by (4.15). By (4.16), $\text{sgn}(\det(K)) = \text{sgn}(\beta)$ because $|\lambda_1|, |\lambda_2| < 1$ in view of $(\tau, \delta) \in \mathcal{T}$.

We now use (4.17) and (4.18) to solve $V(y; z; \mu) = (0, 0)$ for y and z in terms μ . Since V is C^3 and $\det(J) \neq 0$, by the implicit function theorem there exists a unique C^3 solution

$$y^*(\mu) = \frac{\gamma \det(K)}{\alpha a_{12} \omega S_p} \mu + \mathcal{O}(\mu^2), \quad (4.21)$$

$$z^*(\mu) = z_{\text{graz}} + \frac{1}{\alpha a_{12} S_p} (((S_{p+1} - a_{11} S_p)(1 - \alpha) - 1)b_{1p} - a_{12} S_p (1 - \alpha)b_{2p}) \mu + \mathcal{O}(\mu^2), \quad (4.22)$$

for small $\mu \in \mathbb{R}$.

Let $(x^{(0)}(\mu), z^{(0)}(\mu)) = P_{\text{virt}}(R(y^*(\mu), z^*(\mu); \mu); \mu)$, and define $(x^{(j)}(\mu), z^{(j)}(\mu))$ by (4.12) for all $j = 1, 2, \dots, p$. By inserting (4.21)–(4.22) into (4.4), we obtain

$$x^{(0)}(\mu) = \frac{\gamma \phi^2 \det(K)^2}{2\alpha^2 a_{12}^2 \omega^2 S_p^2} \mu^2 + \mathcal{O}(\mu^3), \quad (4.23)$$

$$z^{(0)}(\mu) = z_{\text{graz}} - \frac{b_{1p}}{a_{12} S_p} \mu + \mathcal{O}(\mu^2), \quad (4.24)$$

using the formula (4.15) for $\det(K)$ to achieve simplification in (4.24). Since $(x^{(p)}(\mu), z^{(p)}(\mu)) =$

$P_{\text{virt}}(y^*(\mu), z^*(\mu); \mu)$, we can insert (4.21)–(4.22) into (4.3) to obtain

$$x^{(p)}(\mu) = \frac{\gamma \det(K)^2}{2\alpha^2 a_{12}^2 \omega^2 S_p^2} \mu^2 + \mathcal{O}(\mu^3), \quad (4.25)$$

$$z^{(p)}(\mu) = z_{\text{graz}} + \frac{\det(K) - b_{1p}}{a_{12} S_p} \mu + \mathcal{O}(\mu^2), \quad (4.26)$$

using again (4.15).

Step 2 — Reduce to a linear map.

In order for $(y^*(\mu), z^*(\mu))$ to correspond to a p -loop MPS of (2.3)–(2.5), we require $y^*(\mu) > 0$, and $x^{(j)}(\mu) < 0$ for all $j = 1, 2, \dots, p-1$ so that the periodic solution only hits the wall once per period. By assumption, $a_{12}\alpha > 0$, $\omega > 0$, and $\gamma > 0$. Thus by (4.21) the sign of $\frac{dy^*}{d\mu}(0)$ equals the sign of $\det(K)S_p$, which equals the sign of $\beta\kappa_p$. Thus if $\beta\kappa_p > 0$, then $y^*(\mu) > 0$ for small $\mu > 0$, while if $\beta\kappa_p < 0$, then $y^*(\mu) > 0$ for small $\mu < 0$.

It remains to show that for all $j = 1, 2, \dots, p-1$ the sign of $\frac{dx^{(j)}}{d\mu}(0)$ is opposite to the sign of $\beta\kappa_p$. For all $j = 0, 1, \dots, p$, let

$$(u^{(j)}, w^{(j)}) = \frac{S_p}{\beta} \left(\frac{dx^{(j)}}{d\mu}(0), \frac{dz^{(j)}}{d\mu}(0) \right). \quad (4.27)$$

It remains to show $u^{(j)} < 0$ for all $j = 1, 2, \dots, p-1$ (because $\text{sgn}(S_p) = \text{sgn}(\kappa_p)$).

In view of (2.6) and (4.12), $(u^{(j)}, w^{(j)}) = Q(u^{(j-1)}, w^{(j-1)})$ for all $j = 1, 2, \dots, p$, where Q is the affine map

$$Q(u, w) = A \begin{bmatrix} u \\ w \end{bmatrix} + \frac{S_p}{\beta} b. \quad (4.28)$$

Thus

$$\begin{bmatrix} u^{(j)} \\ w^{(j)} \end{bmatrix} = A^j \begin{bmatrix} u^{(0)} \\ w^{(0)} \end{bmatrix} + \frac{S_p}{\beta} \begin{bmatrix} b_{1j} \\ b_{2j} \end{bmatrix}, \quad (4.29)$$

for all $j = 1, 2, \dots, p$. By (4.23) and (4.24), $u^{(0)} = 0$ and $w^{(0)} = -\frac{b_{1p}}{a_{12}\beta}$. By inserting these and the formulas (4.10) and (4.11) into (4.29) we obtain

$$u^{(j)} = S_p T_j - S_j T_p, \quad (4.30)$$

after simplification.

Step 3 — Verify admissibility.

We first evaluate (4.30) with $j = 1$ and $j = p-1$. Since $S_1 = 1$ and $T_1 = 0$,

$$u^{(1)} = -T_p, \quad (4.31)$$

$$u^{(p-1)} = -\delta^{p-2} H_p(\tau, \delta), \quad (4.32)$$

using also (4.8). By assumption, $\tau > h_p(\delta)$, so $H_p(\tau, \delta) > 0$, by the definition of h_p (see §2.4), and hence $u^{(p-1)} < 0$. Also $\tau > g_{\frac{p}{2}}(\delta)$, by Lemma 2.1, so $T_p > 0$, by Lemma 4.2(c), and hence $u^{(1)} < 0$.

It remains to show $u^{(j)} < 0$ for all $2 \leq j \leq p-2$ when $p \geq 3$. First consider the boundary case $\tau = \delta + 1$ (with $0 < \delta < 1$). Here $\lambda_1 = 1$, $\lambda_2 = \delta$, and $S_j = \frac{1-\delta^j}{1-\delta}$ for each j . So from (4.7), and the formula for a truncated geometric series¹, we obtain $T_p = \frac{p(1-\delta)-(1-\delta^p)}{(1-\delta)^2}$. Then

¹ $\sum_{k=0}^{n-1} r^k = \frac{1-r^n}{1-r}$

by (4.30)

$$u^{(j)} = \frac{j(1 - \delta^p) - p(1 - \delta^j)}{(1 - \delta)^2}, \quad (4.33)$$

which is negative for all $0 < j < p$ (Lemma A.1).

Let \mathcal{P} be the path obtained by linearly connecting $(u^{(0)}, w^{(0)})$ to $(u^{(1)}, w^{(1)})$ to $(u^{(2)}, w^{(2)})$ and so on up to $(u^{(p)}, w^{(p)})$, see Fig. 10. Since $u^{(0)} = u^{(p)} = 0$, \mathcal{P} starts and ends on the w -axis. Since Q is affine, \mathcal{P} has no self intersections and is convex (i.e. the convex hull of \mathcal{P} is equal to the filled polygon with vertices $(u^{(0)}, w^{(0)}), \dots, (u^{(p)}, w^{(p)})$).

We now fix $0 < \delta < 1$ and decrease the value of τ from $\delta + 1$. As we do so, \mathcal{P} varies continuously. Let τ^* be the first value of τ at which $u^{(\ell)} = 0$, for some $1 \leq \ell \leq p - 1$. This cannot occur with $2 \leq \ell \leq p - 2$, for then \mathcal{P} would be non-convex when $\tau = \tau^*$. But $u^{(1)} < 0$ and $u^{(p-1)} < 0$ when $\tau > h_p(\delta)$, thus $\tau^* \leq h_p(\delta)$. Thus for any $h_p(\delta) < \tau < \delta + 1$, we have $u^{(j)} < 0$ for all $2 \leq j \leq p - 2$ as required. \square

5 Calculations for resonant grazing bifurcations

In this section we prove Theorems 2.4 and 2.5 now working with both parameters μ and η .

5.1 Stability of maximal periodic solutions

Consider a p -loop MPS with values y_{imp} and z_{imp} at impact. The stability multipliers of this solution are the eigenvalues of

$$U(y_{\text{imp}}, z_{\text{imp}}; \mu, \eta) = D(P_{\text{global}}^p \circ P_{\text{disc}})(\hat{x}, \hat{z}; \mu, \eta), \quad (5.1)$$

where $(\hat{x}, \hat{z}) = P_{\text{virt}}(y_{\text{imp}}, z_{\text{imp}}; \mu, \eta)$. These eigenvalues are determined by the values of

$$T(y_{\text{imp}}, z_{\text{imp}}; \mu, \eta) = \text{trace}(U(y_{\text{imp}}, z_{\text{imp}}; \mu, \eta)), \quad (5.2)$$

$$D(y_{\text{imp}}, z_{\text{imp}}; \mu, \eta) = \det(U(y_{\text{imp}}, z_{\text{imp}}; \mu, \eta)). \quad (5.3)$$

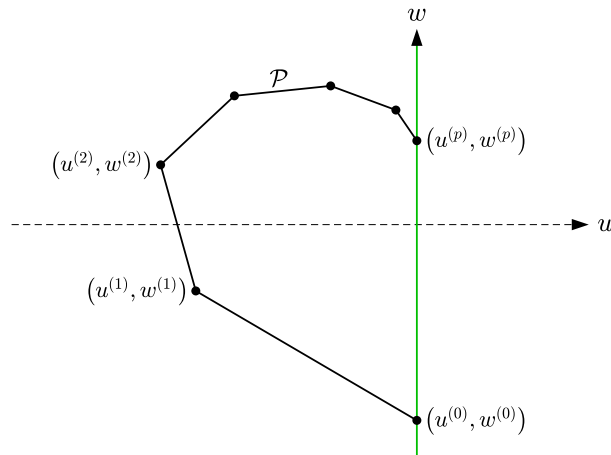


Figure 10: A sketch of the path \mathcal{P} introduced in Step 3 of the proof of Theorem 2.3.

The following results provide asymptotic formulas for T and D . Due to the square-root singularity, we have $T \rightarrow \infty$ as $y_{\text{imp}} \rightarrow 0$. Thus in order to obtain a regular asymptotic expansion, we consider the products $y_{\text{imp}}T$ and $y_{\text{imp}}D$.

We also require some additional notation. In (2.19) we defined

$$\xi_p = \frac{\partial^2 P_{\text{global},1}^p}{\partial z^2} \Big|_{(x,z;\mu,\eta)=(0,z_{\text{graz},0};0,0)},$$

for all $p \geq 1$, and we now also define

$$\begin{aligned} d_p &= \frac{\partial^2 P_{\text{global},1}^p}{\partial z \partial x} \Big|_{(x,z;\mu,\eta)=(0,z_{\text{graz},0};0,0)}, \\ e_p &= \frac{\partial^2 P_{\text{global},1}^p}{\partial z \partial \mu} \Big|_{(x,z;\mu,\eta)=(0,z_{\text{graz},0};0,0)}, \\ f_p &= \frac{\partial^2 P_{\text{global},1}^p}{\partial z \partial \eta} \Big|_{(x,z;\mu,\eta)=(0,z_{\text{graz},0};0,0)}. \end{aligned}$$

For brevity we write $\mathcal{O}(\ell)$ to denote all terms in an expression that are order ℓ or greater.

Lemma 5.1. *Consider a system (2.3)–(2.5) satisfying the assumptions of Theorem 2.4. The products $y_{\text{imp}}T(y_{\text{imp}}, z_{\text{imp}}; \mu, \eta)$ and $y_{\text{imp}}D(y_{\text{imp}}, z_{\text{imp}}; \mu, \eta)$ are well-defined for $y_{\text{imp}} > 0$ and admit C^{k-2} extensions to a neighbourhood of $(y, z; \mu, \eta) = (0, z_{\text{graz},0}; 0, 0)$. Moreover,*

$$\begin{aligned} y_{\text{imp}}T(y_{\text{imp}}, z_{\text{imp}}; \mu, \eta) &= \left(a_{11}\phi^2 + a_{22} - \frac{\alpha\xi_1\omega^2(1-\alpha)}{\gamma} \right) y_{\text{imp}} - \alpha\omega\xi_1(z_{\text{imp}} - z_{\text{graz},0}) \\ &\quad - \alpha\omega e_1\mu - \alpha\omega a'_{12}\eta + \mathcal{O}(2), \end{aligned} \tag{5.4}$$

$$y_{\text{imp}}D(y_{\text{imp}}, z_{\text{imp}}; \mu, \eta) = \phi^2\delta y_{\text{imp}} + \mathcal{O}(2). \tag{5.5}$$

Lemma 5.2. *Consider a system (2.3)–(2.5) satisfying the assumptions of Theorem 2.5. The products $y_{\text{imp}}T(y_{\text{imp}}, z_{\text{imp}}; \mu, \eta)$ and $y_{\text{imp}}D(y_{\text{imp}}, z_{\text{imp}}; \mu, \eta)$ are well-defined for $y_{\text{imp}} > 0$ and admit C^{k-2} extensions to a neighbourhood of $(y, z; \mu, \eta) = (0, z_{\text{graz},0}; 0, 0)$. Moreover,*

$$\begin{aligned} y_{\text{imp}}T(y_{\text{imp}}, z_{\text{imp}}; \mu, \eta) &= - \left((1 + \phi^2)\delta^{\frac{p}{2}} + \frac{\alpha\xi_p\omega^2(1-\alpha)}{\gamma} \right) y_{\text{imp}} - \alpha\omega\xi_p(z_{\text{imp}} - z_{\text{graz},0}) \\ &\quad - \alpha\omega e_p\mu - \alpha\omega f_p\eta + \mathcal{O}(2), \end{aligned} \tag{5.6}$$

$$y_{\text{imp}}D(y_{\text{imp}}, z_{\text{imp}}; \mu, \eta) = \phi^2\delta^p y_{\text{imp}} + \mathcal{O}(2), \tag{5.7}$$

where

$$f_p = \frac{a_{12}p\delta^{\frac{p}{2}-1}\kappa'_p}{2\sin^2\left(\frac{\pi}{p}\right)}. \tag{5.8}$$

Proof of Lemma 5.1. The maps P_{virt} and $P_{\text{virt}} \circ R$ are C^k and given by (4.3) and (4.4). Thus their derivatives are C^{k-1} and given by

$$DP_{\text{virt}}(y_{\text{imp}}, z_{\text{imp}}; \mu, \eta) = \begin{bmatrix} \frac{\partial \hat{x}}{\partial y_{\text{imp}}} & \frac{\partial \hat{x}}{\partial z_{\text{imp}}} \\ \frac{\partial \hat{z}}{\partial y_{\text{imp}}} & \frac{\partial \hat{z}}{\partial z_{\text{imp}}} \end{bmatrix} = \begin{bmatrix} \frac{y_{\text{imp}}}{\gamma} + \mathcal{O}(2) & \mathcal{O}(2) \\ \frac{\omega}{\gamma} + \mathcal{O}(1) & 1 + \mathcal{O}(1) \end{bmatrix}, \quad (5.9)$$

$$D(P_{\text{virt}} \circ R)(y_{\text{imp}}, z_{\text{imp}}; \mu, \eta) = \begin{bmatrix} \frac{\partial x^{(0)}}{\partial y_{\text{imp}}} & \frac{\partial x^{(0)}}{\partial z_{\text{imp}}} \\ \frac{\partial z^{(0)}}{\partial y_{\text{imp}}} & \frac{\partial z^{(0)}}{\partial z_{\text{imp}}} \end{bmatrix} = \begin{bmatrix} \frac{\phi^2 y_{\text{imp}}}{\gamma} + \mathcal{O}(2) & \mathcal{O}(2) \\ \frac{\omega(1-\alpha)}{\gamma} + \mathcal{O}(1) & 1 + \mathcal{O}(1) \end{bmatrix}. \quad (5.10)$$

We have $\det(DP_{\text{virt}}) \rightarrow 0$ as $y_{\text{imp}} \rightarrow 0$, so there exists a C^{k-2} function G_1 such that $\det(DP_{\text{virt}}) = y_{\text{imp}} G_1(y_{\text{imp}}, z_{\text{imp}}; \mu, \eta)$. Moreover, $G_1(0, z_{\text{graz},0}; 0, 0) = \frac{1}{\gamma} \neq 0$ by (5.9), consequently $y_{\text{imp}}(DP_{\text{virt}})^{-1}$ is C^{k-2} (more formally it has a C^{k-2} extension from points with $y_{\text{imp}} > 0$, to a neighbourhood of $(y, z; \mu, \eta) = (0, z_{\text{graz},0}; 0, 0)$). Thus $y_{\text{imp}} DP_{\text{disc}} = y_{\text{imp}} D(P_{\text{virt}} \circ R)(DP_{\text{virt}})^{-1}$ is C^{k-2} , and by (5.9) and (5.10)

$$y_{\text{imp}} DP_{\text{disc}}(y_{\text{imp}}, z_{\text{imp}}; \mu, \eta) = \begin{bmatrix} \phi^2 y_{\text{imp}} + \mathcal{O}(2) & \mathcal{O}(3) \\ -\alpha\omega + \mathcal{O}(1) & y_{\text{imp}} + \mathcal{O}(2) \end{bmatrix}. \quad (5.11)$$

Since $a_{12} = 0$ and $f_1 = a'_{12}$,

$$DP_{\text{global}}(x^{(0)}, z^{(0)}; \mu, \eta) = \begin{bmatrix} a_{11} + \mathcal{O}(1) & d_1 x^{(0)} + \xi_1(z^{(0)} - z_{\text{graz},0}) + e_1 \mu + a'_{12} \eta + \mathcal{O}(2) \\ a_{21} + \mathcal{O}(1) & a_{22} + \mathcal{O}(1) \end{bmatrix}, \quad (5.12)$$

which is C^{k-1} . By multiplying (5.11) and (5.12), and inserting (4.4), we obtain

$$y_{\text{imp}} U(y_{\text{imp}}, z_{\text{imp}}; \mu, \eta) = \begin{bmatrix} X + \mathcal{O}(2) & \mathcal{O}(2) \\ -\alpha\omega a_{22} + \mathcal{O}(1) & a_{22} y_{\text{imp}} + \mathcal{O}(2) \end{bmatrix}, \quad (5.13)$$

where $X = a_{11} \phi^2 y_{\text{imp}} - \alpha\omega \left(\xi_1 \left(\frac{\omega(1-\alpha)}{\gamma} y_{\text{imp}} + z_{\text{imp}} - z_{\text{graz},0} \right) + e_1 \mu + a'_{12} \eta \right)$. By evaluating the trace of (5.13) we obtain (5.4). Also using (5.11) and (5.12) we obtain (5.5). \square

Proof of Lemma 5.2. By assumption $\kappa_p = 0$, i.e. $\tau = g_p(\delta)$. Thus $S_p = 0$ by Lemma 4.2(a), and $S_{p+1} = -\delta^{\frac{p}{2}}$ by Lemma 4.2(b). So from (4.10),

$$DP_{\text{global}}^p(x^{(0)}, z^{(0)}; \mu, \eta) = \begin{bmatrix} -\delta^{\frac{p}{2}} + \mathcal{O}(1) & d_p x^{(0)} + \xi_p(z^{(0)} - z_{\text{graz},0}) + e_p \mu + f_p \eta + \mathcal{O}(2) \\ \mathcal{O}(1) & -\delta^{\frac{p}{2}} + \mathcal{O}(1) \end{bmatrix}, \quad (5.14)$$

which is C^{k-1} because P_{global} is C^k . Also from (4.10), $f_p = a_{12} \frac{\partial S_p}{\partial \eta}$, and it is a simple calculus exercise to verify (5.8) by differentiating (A.11). Following the previous proof, we then multiply (5.11) and (5.14) with (4.4), and take the trace and determine to arrive at (5.6) and (5.7). \square

5.2 Main arguments for resonant grazing bifurcations

Given $p \geq 1$, a p -loop MPS corresponds to a zero of the VIVID function V . At the codimension-two point $(\mu, \eta) = (0, 0)$, the Jacobian matrix J of V , see (4.14), is singular, see (4.15). Thus we cannot directly solve $V(y, z; \mu, \eta) = (0, 0)$ for y and z . However, the

alternate matrix K , see again (4.14), is non-singular, see again (4.15). Thus we can solve $V(y, z; \mu, \eta) = (0, 0)$ for z and μ , at least locally.

Proof of Theorem 2.4. Since $\beta \neq 0$, we have $\det(K) \neq 0$ by (4.15). Thus, by the implicit function theorem, there exist unique C^k functions Z and M such that $V(y, Z(y, \eta); M(y, \eta), \eta) = (0, 0)$ for all (y, η) in a neighbourhood of $(0, 0)$. In view of Assumption 2.2, $Z(0, \eta) = z_{\text{graz}, \eta}$ and $M(0, \eta) = 0$ for all sufficiently small $\eta \in \mathbb{R}$. Also $M(y, \eta)$ is second-order because $\det(J) = 0$. Thus

$$\begin{aligned} Z(y, \eta) &= z_{\text{graz}, \eta} + k_1 y + \mathcal{O}((|y| + |\eta|)^2), \\ M(y, \eta) &= k_2 y^2 + k_3 \eta y + \mathcal{O}((|y| + |\eta|)^3), \end{aligned} \quad (5.15)$$

for some constants $k_1, k_2, k_3 \in \mathbb{R}$.

With $p = 1$, the VIVID function is $V(y, z; \mu, \eta) = (x^{(1)}, z^{(1)}) - (\hat{x}, \hat{z})$. By (2.6) and (5.12), we have

$$\begin{aligned} x^{(1)} &= a_{11}x^{(0)} + b_1\mu + \tilde{\mathcal{O}}(2) + \left(d_1x^{(0)} + e_1\mu + a'_{12}\eta + \tilde{\mathcal{O}}(2)\right)(z^{(0)} - z_{\text{graz}, \eta}) \\ &\quad + \left(\frac{\xi_1}{2} + \tilde{\mathcal{O}}(1)\right)(z^{(0)} - z_{\text{graz}, \eta})^2 + \mathcal{O}\left((z^{(0)} - z_{\text{graz}, \eta})^3\right), \\ z^{(1)} &= z_{\text{graz}, \eta} + a_{21}x^{(0)} + a_{22}(z^{(0)} - z_{\text{graz}, \eta}) + b_2\mu \\ &\quad + \mathcal{O}\left(|x^{(0)}| + |z^{(0)} - z_{\text{graz}, \eta}| + |\mu| + |\eta|\right)^2, \end{aligned} \quad (5.16)$$

using the abbreviation $\tilde{\mathcal{O}}(\ell) = \mathcal{O}\left(|x^{(0)}| + |\mu| + |\eta|\right)^\ell$ for $\ell = 1, 2$. The way in which we have grouped terms in (5.16) is helpful because in the desired result $x^{(0)}$ and μ are higher order than $z^{(0)} - z_{\text{graz}, \eta}$ and η . By substituting (4.4) and (5.15) into (5.16), and then subtracting (4.3), we obtain

$$V(y, Z(y, \eta); M(y, \eta), \eta) = \begin{bmatrix} X_2 y^2 + X_3 \eta y + \mathcal{O}((|y| + |\eta|)^3) \\ X_1 y + \mathcal{O}((|y| + |\eta|)^2) \end{bmatrix},$$

where

$$\begin{aligned} X_1 &= -(1 - a_{22})k_1 + \frac{\omega}{\gamma}(a_{22}(1 - \alpha) - 1), \\ X_2 &= b_1 k_2 + \frac{1}{2\gamma}(a_{11}\phi^2 - 1) + \frac{\xi_1}{2} \left(k_1 + \frac{(1 - \alpha)\omega}{\gamma}\right)^2, \\ X_3 &= b_1 k_3 + a'_{12} \left(k_1 + \frac{(1 - \alpha)\omega}{\gamma}\right). \end{aligned}$$

To have $V(y, Z(y, \eta); M(y, \eta), \eta) = (0, 0)$, we require $X_i = 0$ for all $i = 1, 2, 3$, thus

$$k_1 = \frac{\omega(a_{22}(1 - \alpha) - 1)}{(1 - a_{22})\gamma}, \quad k_2 = \frac{-s_1^+}{2(1 - a_{22})b_1\gamma}, \quad k_3 = \frac{\alpha\omega a'_{12}}{(1 - a_{22})b_1\gamma}, \quad (5.17)$$

using the formula (2.20) for s_1^+ .

Now define

$$\Psi^\pm(y, \eta) = T(y, Z(y, \eta); M(y, \eta), \eta) \mp D(y, Z(y, \eta); M(y, \eta), \eta) \mp 1. \quad (5.18)$$

The one-loop MPS has a stability multiplier of 1 when $\Psi^+(y, \eta) = 0$, and a stability multiplier of -1 when $\Psi^-(y, \eta) = 0$. By Lemma 5.1, the product $y\Psi^\pm(y, \eta)$ is C^{k-2} . By inserting (5.15) with (5.17) into (5.4) and (5.5) we obtain (after some algebraic manipulation),

$$y\Psi^\pm(y, \eta) = s_1^\pm y - \alpha\omega a'_{12}\eta + \mathcal{O}((|y| + |\eta|)^2),$$

using again (2.20). Since $s_1^\pm \neq 0$, by the implicit function theorem there exists a unique C^{k-2} function $\Upsilon^\pm(\eta)$ such that $\Upsilon^\pm(\eta)\Psi^\pm(\Upsilon^\pm(\eta), \eta) = 0$ for all η in a neighbourhood of 0, and

$$\Upsilon^\pm(\eta) = \frac{\alpha\omega a'_{12}}{s_1^\pm} \eta + \mathcal{O}(\eta^2). \quad (5.19)$$

Let $g_{\text{SN},1}(\eta) = M(\Upsilon^+(\eta), \eta)$ and $g_{\text{PD},1}(\eta) = M(\Upsilon^+(\eta), \eta)$. These functions are C^{k-2} , and from (5.17) and (5.19) we obtain (2.21) after simplification. Notice $k_2 \neq 0$ by (5.17), so the coefficient of the y^2 -term in (5.15) is non-zero. Thus as we move away from $\mu = g_{\text{SN},1}(\eta)$ by perturbing the value of μ in the appropriate direction, two zeros of the VIVID function separate from one another at a rate asymptotically proportional to the square root of the change in μ . Therefore $\mu = g_{\text{SN},1}(\eta)$ is a curve of saddle-node bifurcations. With $\text{sgn}(\eta) = \text{sgn}(a'_{12}s_1^\pm)$, the impact velocity $\Upsilon^\pm(\eta)$ of the one-loop MPS is positive for sufficiently small $\eta \neq 0$ by (5.19), and because $\alpha > 0$ and $\omega > 0$. Thus for this sign of η the one-loop MPS is admissible. \square

Proof of Theorem 2.5. As in the previous proof there exist unique C^k functions Z and M of the form (5.15) such that $V(y, Z(y, \eta); M(y, \eta), \eta) = (0, 0)$ for all (y, η) in a neighbourhood of $(0, 0)$. By (4.9)–(4.11) and (5.14),

$$\begin{aligned} x^{(p)} &= -\delta^{\frac{p}{2}}x^{(0)} + T_p\beta\mu + \tilde{\mathcal{O}}(2) + \left(d_px^{(0)} + e_p\mu + f_p\eta + \tilde{\mathcal{O}}(2)\right)(z^{(0)} - z_{\text{graz},\eta}) \\ &\quad + \left(\frac{\xi_p}{2} + \tilde{\mathcal{O}}(1)\right)(z^{(0)} - z_{\text{graz},\eta})^2 + \mathcal{O}\left((z^{(0)} - z_{\text{graz},\eta})^3\right), \\ z^{(p)} &= z_{\text{graz},\eta} - \delta^{\frac{p}{2}}(z^{(0)} - z_{\text{graz},\eta}) + T_p(a_{21}b_1 + (1 - a_{11})b_2)\mu \\ &\quad + \mathcal{O}\left((|x^{(0)}| + |z^{(0)} - z_{\text{graz},\eta}| + |\mu| + |\eta|)^2\right). \end{aligned} \quad (5.20)$$

By substituting (4.4) and (5.15) into (5.20), and then subtracting (4.3), we obtain

$$V(y, Z(y, \eta); M(y, \eta), \eta) = \begin{bmatrix} X_2y^2 + X_3\eta y + \mathcal{O}((|y| + |\eta|)^3) \\ X_1y + \mathcal{O}((|y| + |\eta|)^2) \end{bmatrix},$$

where

$$\begin{aligned} X_1 &= -\left(1 + \delta^{\frac{p}{2}}\right)k_1 - \frac{\omega}{\gamma}\left(1 + \delta^{\frac{p}{2}}(1 - \alpha)\right), \\ X_2 &= T_p\beta k_2 - \frac{1}{2\gamma}\left(1 + \delta^{\frac{p}{2}}\phi^2\right) + \frac{\xi_p}{2}\left(k_1 + \frac{(1 - \alpha)\omega}{\gamma}\right)^2, \\ X_3 &= T_p\beta k_3 + f_p\left(k_1 + \frac{(1 - \alpha)\omega}{\gamma}\right). \end{aligned}$$

Solving $X_i = 0$ for all $i = 1, 2, 3$, gives

$$k_1 = -\frac{\omega(1 + \delta^{\frac{p}{2}}(1 - \alpha))}{(1 + \delta^{\frac{p}{2}})\gamma}, \quad k_2 = \frac{-s_p^+}{2(1 + \delta^{\frac{p}{2}})\beta\gamma T_p}, \quad k_3 = \frac{\alpha\omega f_p}{(1 + \delta^{\frac{p}{2}})\beta\gamma T_p}, \quad (5.21)$$

using (2.24). By inserting (5.15) with (5.21) into (5.6) and (5.7), we obtain

$$y\Psi^\pm(y, \eta) = s_p^\pm y - \alpha\omega f_p \eta + \mathcal{O}((|y| + |\eta|)^2),$$

using again (2.24). Since $s_p^\pm \neq 0$, by the implicit function theorem there exists a unique C^{k-2} function $\Upsilon^\pm(\eta)$ such that $\Upsilon^\pm(\eta)\Psi^\pm(\Upsilon^\pm(\eta), \eta) = 0$ for all η in a neighbourhood of 0, and

$$\Upsilon^\pm(\eta) = \frac{\alpha\omega f_p}{s_p^\pm} \eta + \mathcal{O}(\eta^2). \quad (5.22)$$

Let $g_{\text{SN},p}(\eta) = M(\Upsilon^+(\eta), \eta)$ and $g_{\text{PD},p}(\eta) = M(\Upsilon^-(\eta), \eta)$. These functions are C^{k-2} , and from (5.21) and (5.22) we obtain (2.25), using also Lemma 4.2 and (5.8) for T_p and f_p . As in the previous proof, $\mu = g_{\text{SN},p}(\eta)$ is a curve of saddle-node bifurcations because the coefficient of the y^2 -term in (5.15) is non-zero by (5.21).

Finally, we show that on the bifurcation curves $\mu = g_{\text{SN},p}(\eta)$ and $\mu = g_{\text{PD},p}(\eta)$, the p -loop MPS is admissible for sufficiently small $\eta \neq 0$ with $\text{sgn}(\eta) = \text{sgn}(\kappa'_p s_p^\pm)$. Observe $\text{sgn}(f_p) = \text{sgn}(a_{12}\kappa'_p)$, by (5.8). So by (5.22), $\text{sgn}(\Upsilon^\pm(\eta)) = \text{sgn}(\alpha a_{12}\kappa'_p s_p^\pm \eta)$, for sufficiently small $\eta \neq 0$. Thus $\text{sgn}(\eta) = \text{sgn}(\kappa'_p s_p^\pm)$ ensures that the impact velocity $y^*(\eta) = \Upsilon^\pm(\eta)$ of the p -loop MPS is positive for sufficiently small $\eta \neq 0$.

On the bifurcation curve, the z -value of the p -loop MPS at impact is

$$z^*(\eta) = Z(\Upsilon^\pm(\eta), \eta) = z_{\text{graz},\eta} + \frac{\alpha\omega f_p k_1}{s_p^\pm} \eta + \mathcal{O}(\eta^2), \quad (5.23)$$

by (5.15) and (5.22). Analogous to the proof of Theorem 2.3, let $(x^{(0)}(\eta), z^{(0)}(\eta)) = P_{\text{virt}}(R(y^*(\eta), z^*(\eta)))$ and $(x^{(j)}(\eta), z^{(j)}(\eta)) = P_{\text{global}}(x^{(j-1)}, z^{(j-1)})$ for all $j = 1, 2, \dots, p$. Trivially, $x^{(0)}(\eta) > 0$ and $x^{(p)}(\eta) > 0$, by (4.3) and (4.4), so it remains to show $x^{(j)}(\eta) < 0$ for all $j = 1, 2, \dots, p - 1$ and sufficiently small $\eta \neq 0$ with $\text{sgn}(\eta) = \text{sgn}(\kappa'_p s_p^\pm)$.

By (4.4) and (5.23),

$$x^{(0)}(\eta) = \mathcal{O}(\eta^2), \quad (5.24)$$

$$\begin{aligned} z^{(0)}(\eta) &= z_{\text{graz},\eta} + \frac{\alpha\omega f_p}{s_p^\pm} \left(k_1 + \frac{\omega(1-\alpha)}{\gamma}\right) \eta + \mathcal{O}(\eta^2) \\ &= z_{\text{graz},\eta} - \frac{\alpha^2\omega^2 f_p}{\gamma(1 + \delta^{\frac{p}{2}})s_p^\pm} \eta + \mathcal{O}(\eta^2), \end{aligned} \quad (5.25)$$

using also (5.21). On the bifurcation curve, $\mu = M(\Upsilon^\pm(\eta), \eta) = \mathcal{O}(\eta^2)$, so the constant term in P_{global} is second-order, and hence to first order we have simply

$$\begin{bmatrix} x^{(j)}(\eta) \\ z^{(j)}(\eta) \end{bmatrix} = \begin{bmatrix} 0 \\ z_{\text{graz}, \eta} \end{bmatrix} + A^j \begin{bmatrix} x^{(0)}(\eta) \\ z^{(0)}(\eta) - z_{\text{graz}, \eta} \end{bmatrix} + \mathcal{O}(\eta^2). \quad (5.26)$$

By (4.10), the (1, 2)-entry of A^j is $a_{12}S_j$, so by substituting (5.24) and (5.25) into (5.26) we obtain

$$x^{(j)}(\eta) = -\frac{a_{12}S_j\alpha^2\omega^2 f_p}{\gamma(1 + \delta^{\frac{p}{2}})s_p^\pm} \eta + \mathcal{O}(\eta^2). \quad (5.27)$$

By (5.8), $\text{sgn}(f_p) = \text{sgn}(a_{12}\kappa'_p)$. Also $S_j > 0$, for all $j = 1, 2, \dots, p-1$, because at resonance $\theta = \frac{\pi}{p}$ in (A.11). So (5.27) implies

$$\text{sgn}(x^{(j)}(\eta)) = -\text{sgn}(\kappa'_p s_p^\pm \eta), \quad (5.28)$$

for sufficiently small $\eta \neq 0$. Hence with $\text{sgn}(\eta) = \text{sgn}(\kappa'_p s_p^\pm)$, we have $x^{(j)}(\eta) < 0$ for all $j = 1, 2, \dots, p-1$ as required. \square

6 Discussion

Grazing bifurcations elicit a severe nonlinearity, so often induce a chaotic response. Yet, the response can be periodic, due to the presence of resonant grazing bifurcations. We have performed the first formal unfolding of resonant grazing bifurcations to explain how these initiate periodicity regions bounded by curves of saddle-node and period-doubling bifurcations. We have obtained explicit formulas for the coefficients of the leading-order (quadratic) terms of these curves. The formulas are valuable as they reveal the direction and shape of the curves as they emanate from the resonant grazing bifurcation. For example, for the linear impact oscillator model, the curves emanate in different directions for different $p = 1$ resonant grazing bifurcations. Theorem 2.4 shows how the direction is governed by the sign of a'_{12} , and Proposition 3.2 shows how the sign of a'_{12} is determined by the parity of n . This explains why in Fig. 7 the geometry of the $p = 1$ periodicity region with resonant point at $\omega \approx 0.5$ is starkly different to the geometries of the other periodicity regions. This region corresponds to $n = 4$, while the other $p = 1$ regions correspond to $n = 3$ and $n = 5$.

The theorems in §2 apply to any impact oscillator model that can be put in the form (2.3)–(2.5). For a nonlinear oscillator, the quantities in the theorems can be evaluated by simulating the Poincaré map P_{global} numerically, and evaluating its derivatives through finite difference approximations. The theorems can also be applied to grazing bifurcations of periodic solutions that have impacts at other parts of their trajectories, as these impacts do not affect the smoothness of P_{global} .

It remains to determine if there is a simple criterion that dictates the criticality of the period-doubling bifurcations. All of the period-doubling bifurcations that we have identified for the linear impact oscillator model appear to be subcritical, i.e. create an unstable period-doubled solution. Each period-doubled solution undergoes grazing along another bifurcation curve emanating from the resonant grazing bifurcation. We have not computed these curves

as they do not bound the periodicity regions, and an asymptotic computation of these curves is beyond the scope of this work. The inclusion of these curves would bring the unfolding closer to that of a *homoclinic-doubling bifurcation*: codimension-two points on curves of homoclinic bifurcations from which there issue curves of saddle-node, period-doubling, and homoclinic bifurcations of the period-doubled solution [38–40]. It is not yet clear why resonant grazing and homoclinic-doubling bifurcations admit similar unfoldings. Homoclinic-doubling bifurcations often appear in cascades, which is not what we see for resonant grazing bifurcations, but is reminiscent of cascades of grazing-sliding bifurcations. These result from boundary equilibrium bifurcations with homoclinic or heteroclinic connections [41, pg. 373], and yet to be fully explained.

Acknowledgements

This work was supported by Marsden Fund contract MAU2209 managed by Royal Society Te Apārangi. The authors thank John Bailie and Soumitro Banerjee for helpful conversations.

A Additional calculations regarding the eigenvalues of A

By definition,

$$H_p(\tau, \delta) = \sum_{j=1}^{p-1} \sum_{k=1}^j \lambda_1^{k-j} \lambda_2^{1-k}, \quad (\text{A.1})$$

repeating (2.16). Since $0 < \delta < 1$, we have $\lambda_1, \lambda_2 \neq 0$, $\lambda_2 \neq 1$, and

$$\lambda_1 = 1 \text{ if and only if } \tau = \delta + 1, \text{ and}$$

$$\lambda_1 = \lambda_2 \text{ if and only if } \tau = 2\sqrt{\delta}.$$

If $\tau \neq \delta + 1$ and $\tau \neq 2\sqrt{\delta}$, then by three applications of the formula for the sum of a truncated geometric series,

$$H_p(\tau, \delta) = \frac{\lambda_1 \lambda_2}{\lambda_1 - \lambda_2} \sum_{j=1}^{p-1} (\lambda_2^{-j} - \lambda_1^{-j}) \quad (\text{A.2})$$

$$\begin{aligned} &= \frac{\lambda_1 \lambda_2}{\lambda_1 - \lambda_2} \left(\frac{\lambda_2^{p-1} - 1}{\lambda_2^{p-1}(\lambda_2 - 1)} - \frac{\lambda_1^{p-1} - 1}{\lambda_1^{p-1}(\lambda_1 - 1)} \right) \\ &= \frac{\lambda_1^{p-1} \lambda_2^{p-1} (\lambda_1 - \lambda_2) - (\lambda_1^p - \lambda_2^p) + (\lambda_1^{p-1} - \lambda_2^{p-1})}{(1 - \lambda_1)(1 - \lambda_2)(\lambda_1 - \lambda_2) \lambda_1^{p-2} \lambda_2^{p-2}}. \end{aligned} \quad (\text{A.3})$$

In a similar fashion we obtain from (4.7),

$$T_p = \frac{1}{\lambda_1 - \lambda_2} \sum_{j=1}^{p-1} (\lambda_1^j - \lambda_2^j) \quad (\text{A.4})$$

$$= \frac{\lambda_1 - \lambda_2 - (\lambda_1^p - \lambda_2^p) + \lambda_1 \lambda_2 (\lambda_1^{p-1} - \lambda_2^{p-1})}{(1 - \lambda_1)(1 - \lambda_2)(\lambda_1 - \lambda_2)}. \quad (\text{A.5})$$

Proof of Lemma 2.1. If $\tau \geq 2\sqrt{\delta}$, then λ_1 and λ_2 are real and positive, so by (A.1), $H_p(\tau, \delta) > 0$ for all $\tau \geq 2\sqrt{\delta}$.

Thus for the remainder of the proof it suffices to consider $g_{\frac{p}{2}}(\delta) \leq \tau < 2\sqrt{\delta}$, with which λ_1 and λ_2 are complex-valued. In this case

$$\lambda_1 = r e^{i\theta}, \quad \lambda_2 = r e^{-i\theta}, \quad (\text{A.6})$$

where $r = \sqrt{\delta}$ and $\theta = \cos^{-1}\left(\frac{\tau}{2\sqrt{\delta}}\right) \in (0, \pi)$. For any $k \in \mathbb{Z}$, we have

$$\lambda_1^k - \lambda_2^k = 2ir^k \sin(k\theta), \quad (\text{A.7})$$

thus by (A.2)

$$H_p(\tau, \delta) = \frac{1}{\sin(\theta)} \sum_{j=1}^{p-1} r^{1-j} \sin(j\theta). \quad (\text{A.8})$$

Thus $H_p(\tau, \delta) > 0$ for all $\theta \in \left(0, \frac{\pi}{p-1}\right]$, which is equivalent to $\tau \in \left[g_{p-1}(\delta), 2\sqrt{\delta}\right)$.

By instead inserting (A.7) into (A.3), we obtain

$$H_p(\tau, \delta) = \frac{r^p \sin(\theta) - r \sin(p\theta) + \sin((p-1)\theta)}{(\delta - \tau + 1)r^{p-2} \sin(\theta)}. \quad (\text{A.9})$$

By substituting $\theta = \frac{2\pi}{p}$ into (A.9) (possible because $p \geq 3$), we obtain (after simplification)

$$H_p\left(g_{\frac{p}{2}}(\delta), \delta\right) = \frac{r^p - 1}{(\delta - \tau + 1)r^{p-2}} < 0,$$

using also $r < 1$. In summary, we have shown $H_p\left(g_{\frac{p}{2}}(\delta), \delta\right) < 0$ and $H_p(\tau, \delta) > 0$, for all $\tau \geq g_{p-1}(\delta)$. Thus, by the intermediate value theorem, there exists $\tau^* \in \left(g_{\frac{p}{2}}(\delta), g_{p-1}(\delta)\right)$ such that $H_p(\tau^*, \delta) = 0$, and $h_p(\delta)$ is the largest such τ^* . \square

Proof of Lemma 4.2(a). If $\tau \geq 2\sqrt{\delta}$, then λ_1 and λ_2 are real and positive, and by (4.7) we have $S_p > 0$. Thus it suffices to assume $\tau < 2\sqrt{\delta}$, with which the eigenvalues can be written in the form (A.6). Also $\lambda_1 \neq \lambda_2$, so

$$S_p = \frac{\lambda_1^p - \lambda_2^p}{\lambda_1 - \lambda_2}. \quad (\text{A.10})$$

For any $k \in \mathbb{Z}$, $\lambda_1^k - \lambda_2^k = 2ir^k \sin(k\theta)$, thus

$$S_p = \frac{r^{p-1} \sin(p\theta)}{\sin(\theta)}. \quad (\text{A.11})$$

Thus $S_p = 0$ if and only if $\theta = \frac{m\pi}{p}$ for some $m = 1, 2, \dots, p-1$; equivalently $\tau = g_{\frac{p}{m}}(\delta)$ for some $m = 1, 2, \dots, p-1$. But we cannot have $\tau = g_{\frac{p}{m}}(\delta)$ for any $m \geq 2$ because $\tau > h_p(\delta)$ and $h_p(\delta) > g_{\frac{p}{2}}(\delta)$ by Lemma 2.1. \square

Proof of Lemma 4.2(b). By (A.11), $S_{p+1} = \frac{r^p \sin((p+1)\theta)}{\sin(\theta)}$, where $\sin((p+1)\theta) = \sin(p\theta) \cos(\theta) + \cos(p\theta) \sin(\theta)$. With $\tau = g_p(\delta)$, we have $\theta = \frac{\pi}{p}$ by the definition (2.15) of g_p , so $\sin(p\theta) = 0$ and $\cos(p\theta) = -1$. Thus $S_{p+1} = -r^p = -\delta^{\frac{p}{2}}$.

By (A.5) and (A.7)

$$T_p = \frac{\sin(\theta) - r^{p-1} \sin(p\theta) + r^p \sin((p-1)\theta)}{(\delta - \tau + 1) \sin(\theta)}. \quad (\text{A.12})$$

But $\tau = g_p(\delta)$, so $\sin(p\theta) = 0$ and $\cos(p\theta) = -1$, and hence $\sin((p-1)\theta) = \sin(p\theta) \cos(\theta) - \cos(p\theta) \sin(\theta) = \sin(\theta)$. Thus $T_p = \frac{1+\delta^{\frac{p}{2}}}{\delta-\tau+1}$ because $r = \sqrt{\delta}$. \square

Proof of Lemma 4.2(c). Since $T_2 = 1$, we can assume $p \geq 3$. If $\tau \geq 2\sqrt{\delta}$, then λ_1 and λ_2 are real and positive, so $T_p > 0$ by (4.7).

So it remains to consider $g_{\frac{p}{2}}(\delta) \leq \tau < 2\sqrt{\delta}$ and use the polar form (A.6). By (A.4) and (A.7),

$$T_p = \frac{1}{\sin(\theta)} \sum_{j=1}^{p-1} r^{j-1} \sin(j\theta). \quad (\text{A.13})$$

With $0 < \theta < \frac{\pi}{p-1}$ (equivalently $g_{p-1}(\delta) < \tau < 2\sqrt{\delta}$), each term in (A.13) is positive, hence $T_p > 0$.

So it remains to consider $\frac{\pi}{p-1} \leq \theta \leq \frac{2\pi}{p}$. The formula (A.12) can be rewritten as

$$T_p = \frac{r^{p-1} \Xi(\theta) - r^{p-1} (1-r) \sin((p-1)\theta) + (1-r^{p-1}) \sin(\theta)}{(\delta - \tau + 1) \sin(\theta)}, \quad (\text{A.14})$$

where

$$\Xi(\theta) = \sin(\theta) - \sin(p\theta) + \sin((p-1)\theta).$$

By various trigonometric identities, this can be factored as

$$\Xi(\theta) = 4 \sin\left(\frac{\theta}{2}\right) \sin\left(\frac{(p-1)\theta}{2}\right) \sin\left(\frac{p\theta}{2}\right).$$

Thus $\theta \leq \frac{2\pi}{p}$ implies $\Xi(\theta) \geq 0$, so the first term in the numerator of (A.14) is greater than or equal to zero. The second term in the numerator is also greater than or equal to zero because $\frac{\pi}{p-1} \leq \theta \leq \frac{2\pi}{p}$. The third term in the numerator is strictly greater than zero, thus $T_p > 0$. \square

Lemma A.1. *Let $0 < \delta < 1$, $p \geq 1$, and $0 < j < p$. Then*

$$j(1 - \delta^p) - p(1 - \delta^j) < 0. \quad (\text{A.15})$$

Proof. The line tangent to $f(x) = x^{\frac{j}{p}}$ at $x = 1$ is $f_{\text{tang}}(x) = 1 + \frac{j}{p}(x - 1)$. Since $f(x)$ is concave down, $f(x) < f_{\text{tang}}(x)$ for all $0 < x < 1$. Substituting $x = \delta^p$ into $f(x) < f_{\text{tang}}(x)$ gives

$$\delta^j < 1 + \frac{j}{p}(\delta^p - 1),$$

which is equivalent to (A.15). \square

B Calculations for the linear impact oscillator

Proof of Proposition 3.1. Here we derive (3.9) and (3.10). Write $(x', z') = P_{\text{global}}(x, z; \mathcal{A} - \mathcal{A}_{\text{graz}}(\omega))$. This map corresponds to an orbit in (x, y) -phase space that starts at $(x, 0)$ at time $\frac{z}{\omega}$, and ends at $(x', 0)$ at time $\frac{z'+2\pi}{\omega}$. The orbit is given explicitly as $(\phi, \dot{\phi})$, so

$$\begin{aligned} x' &= \phi\left(\frac{z'+2\pi}{\omega}; x, 0, \frac{z}{\omega}; \mathcal{A}\right), \\ 0 &= \dot{\phi}\left(\frac{z'+2\pi}{\omega}; x, 0, \frac{z}{\omega}; \mathcal{A}\right). \end{aligned} \quad (\text{B.1})$$

At grazing, i.e. with $(x, z; \mathcal{A}) = (0, z_{\text{graz}}; \mathcal{A}_{\text{graz}}(\omega))$, we map to $(x', z') = (0, z_{\text{graz}})$. Given suitably small $\delta_1, \delta_2, \delta_3 \in \mathbb{R}$, with the perturbed values $(x, z; \mathcal{A}) = (\delta_1, z_{\text{graz}} + \delta_2; \mathcal{A}_{\text{graz}}(\omega) + \delta_3)$, we map to $(x', z') = (a_{11}\delta_1 + a_{12}\delta_2 + b_1\delta_3 + \mathcal{O}(2), z_{\text{graz}} + a_{21}\delta_1 + a_{22}\delta_2 + b_2\delta_3 + \mathcal{O}(2))$, where $\mathcal{O}(2)$ denotes terms that are quadratic or higher order in δ_1, δ_2 , and δ_3 . By substituting these into (B.1) and Taylor expanding ϕ and $\dot{\phi}$ to first order, we obtain

$$\begin{aligned} a_{11}\delta_1 + a_{12}\delta_2 + b_1\delta_3 &= \dot{\phi} \frac{(a_{21}\delta_1 + a_{22}\delta_2 + b_2\delta_3)}{\omega} + \frac{\partial\phi}{\partial x} \delta_1 + \frac{\partial\phi}{\partial t_0} \frac{\delta_2}{\omega} + \frac{\partial\phi}{\partial \mathcal{A}} \delta_3 + \mathcal{O}(2), \\ 0 &= \ddot{\phi} \frac{(a_{21}\delta_1 + a_{22}\delta_2 + b_2\delta_3)}{\omega} + \frac{\partial\dot{\phi}}{\partial x} \delta_1 + \frac{\partial\dot{\phi}}{\partial t_0} \frac{\delta_2}{\omega} + \frac{\partial\dot{\phi}}{\partial \mathcal{A}} \delta_3 + \mathcal{O}(2), \end{aligned} \quad (\text{B.2})$$

where each quantity involving ϕ is evaluated at grazing. Matching terms in (B.2) gives

$$\begin{aligned} a_{11} &= \frac{\partial\phi}{\partial x} - \frac{\dot{\phi}}{\ddot{\phi}} \frac{\partial\dot{\phi}}{\partial x}, & a_{12} &= \frac{1}{\omega} \left(\frac{\partial\phi}{\partial t_0} - \frac{\dot{\phi}}{\ddot{\phi}} \frac{\partial\dot{\phi}}{\partial t_0} \right), \\ a_{21} &= -\frac{\omega}{\ddot{\phi}} \frac{\partial\dot{\phi}}{\partial x}, & a_{22} &= -\frac{1}{\dot{\phi}} \frac{\partial\dot{\phi}}{\partial t_0}, \\ b_1 &= \frac{\partial\phi}{\partial \mathcal{A}} - \frac{\dot{\phi}}{\ddot{\phi}} \frac{\partial\dot{\phi}}{\partial \mathcal{A}}, & b_2 &= -\frac{\omega}{\dot{\phi}} \frac{\partial\dot{\phi}}{\partial \mathcal{A}}, \end{aligned} \quad (\text{B.3})$$

where again each quantity involving ϕ is evaluated at grazing. By differentiating the explicit expressions (3.3) and (3.4), and evaluating these at grazing, we obtain

$$\begin{aligned}
\dot{\phi} &= 0, & \ddot{\phi} &= -\omega^2, \\
\frac{\partial \phi}{\partial x} &= e^{-\frac{2\pi\zeta}{\omega}} \left(\cos\left(\frac{2\pi\omega_1}{\omega}\right) + \frac{\zeta}{\omega_1} \sin\left(\frac{2\pi\omega_1}{\omega}\right) \right), & \frac{\partial \dot{\phi}}{\partial x} &= -\frac{1}{\omega_1} e^{-\frac{2\pi\zeta}{\omega}} \sin\left(\frac{2\pi\omega_1}{\omega}\right), \\
\frac{\partial \phi}{\partial t_0} &= \frac{\omega^2}{\omega_1} e^{-\frac{2\pi\zeta}{\omega}} \sin\left(\frac{2\pi\omega_1}{\omega}\right), & \frac{\partial \dot{\phi}}{\partial t_0} &= \omega^2 e^{-\frac{2\pi\zeta}{\omega}} \left(\cos\left(\frac{2\pi\omega_1}{\omega}\right) - \frac{\zeta}{\omega_1} \sin\left(\frac{2\pi\omega_1}{\omega}\right) \right), \\
\frac{\partial \phi}{\partial \mathcal{A}} &= \frac{1 - e^{-\frac{2\pi\zeta}{\omega}} \left(\cos\left(\frac{2\pi\omega_1}{\omega}\right) + \frac{\zeta}{\omega_1} \sin\left(\frac{2\pi\omega_1}{\omega}\right) \right)}{\mathcal{A}_{\text{graz}}(\omega)}, & \frac{\partial \dot{\phi}}{\partial \mathcal{A}} &= \frac{e^{-\frac{2\pi\zeta}{\omega}} \sin\left(\frac{2\pi\omega_1}{\omega}\right)}{\omega_1 \mathcal{A}_{\text{graz}}(\omega)}.
\end{aligned} \tag{B.4}$$

By substituting these into (B.3), we obtain

$$\begin{aligned}
a_{11} &= e^{-\frac{2\pi\zeta}{\omega}} \left(\cos\left(\frac{2\pi\omega_1}{\omega}\right) + \frac{\zeta}{\omega_1} \sin\left(\frac{2\pi\omega_1}{\omega}\right) \right), & a_{12} &= \frac{\omega}{\omega_1} e^{-\frac{2\pi\zeta}{\omega}} \sin\left(\frac{2\pi\omega_1}{\omega}\right), \\
a_{21} &= -\frac{1}{\omega_1 \omega} e^{-\frac{2\pi\zeta}{\omega}} \sin\left(\frac{2\pi\omega_1}{\omega}\right), & a_{22} &= e^{-\frac{2\pi\zeta}{\omega}} \left(\cos\left(\frac{2\pi\omega_1}{\omega}\right) - \frac{\zeta}{\omega_1} \sin\left(\frac{2\pi\omega_1}{\omega}\right) \right), \\
b_1 &= \frac{1 - e^{-\frac{2\pi\zeta}{\omega}} \left(\cos\left(\frac{2\pi\omega_1}{\omega}\right) + \frac{\zeta}{\omega_1} \sin\left(\frac{2\pi\omega_1}{\omega}\right) \right)}{\mathcal{A}_{\text{graz}}(\omega)}, & b_2 &= \frac{e^{-\frac{2\pi\zeta}{\omega}} \sin\left(\frac{2\pi\omega_1}{\omega}\right)}{\omega_1 \omega \mathcal{A}_{\text{graz}}(\omega)},
\end{aligned}$$

which are the desired formulas (3.9) and (3.10). \square

Proof of Proposition 3.2. By extending the asymptotic calculations of the previous proof from first-order to second-order, we obtain

$$\xi_1 = \frac{1}{\omega^2} \left(a_{22}^2 \left(\ddot{\phi} - \frac{\dot{\phi} \ddot{\phi}}{\dot{\phi}} \right) + 2a_{22} \left(\frac{\partial \dot{\phi}}{\partial t_0} - \frac{\dot{\phi}}{\dot{\phi}} \frac{\partial \ddot{\phi}}{\partial t_0} \right) + \frac{\partial^2 \phi}{\partial t_0^2} - \frac{\dot{\phi}}{\dot{\phi}} \frac{\partial^2 \dot{\phi}}{\partial t_0^2} \right).$$

At grazing

$$\frac{\partial^2 \phi}{\partial t_0^2} = -\omega^2 e^{-\frac{2\pi\zeta}{\omega}} \left(\cos\left(\frac{2\pi\omega_1}{\omega}\right) - \frac{3\zeta}{\omega_1} \sin\left(\frac{2\pi\omega_1}{\omega}\right) \right), \tag{B.5}$$

and by also using the formulas (B.4), we obtain

$$\xi_1 = e^{-\frac{4\pi\zeta}{\omega}} \left(\cos\left(\frac{2\pi\omega_1}{\omega}\right) - \frac{\zeta}{\omega_1} \sin\left(\frac{2\pi\omega_1}{\omega}\right) \right)^2 - e^{-\frac{2\pi\zeta}{\omega}} \left(\cos\left(\frac{2\pi\omega_1}{\omega}\right) - \frac{3\zeta}{\omega_1} \sin\left(\frac{2\pi\omega_1}{\omega}\right) \right). \tag{B.6}$$

At resonance, $\sin\left(\frac{2\pi\omega_1}{\omega}\right) = \sin(n\pi) = 0$, and $\cos\left(\frac{2\pi\omega_1}{\omega}\right) = \cos(n\pi) = (-1)^n$, so (B.6) reduces to

$$\xi_1 = E_1(E_1 - (-1)^n), \tag{B.7}$$

where $E_1 = e^{-\frac{2\pi\zeta}{\omega}}$. Also $a_{11} = a_{22} = (-1)^n E_1$, so by evaluating (2.20) we obtain

$$\begin{aligned}
s_1^\pm &= (1 \mp (-1)^n E_1) \left((-1)^n \epsilon^2 E_1 \mp 1 \right) + \frac{(1 + \epsilon)^2 E_1 (E_1 - (-1)^n)}{1 - (-1)^n E_1} \\
&= \mp \left(1 \pm 2(-1)^n \epsilon E_1 + \epsilon^2 E_1^2 \right),
\end{aligned} \tag{B.8}$$

using also (3.7) and (3.8). This verifies the formulas for s_1^\pm in (3.15) and (3.16).

For the impact oscillator we are using $\eta = \omega - \omega^*$, so $a'_{12} = \frac{\partial a_{12}}{\partial \omega}$, evaluated at grazing. By differentiating $a_{12} = \frac{\omega}{\omega_1} e^{-\frac{2\pi\zeta}{\omega}} \sin\left(\frac{2\pi\omega_1}{\omega}\right)$ with respect to ω , we obtain

$$a'_{12} = -\frac{2\pi(-1)^n E_1}{\omega}, \quad (\text{B.9})$$

using again $\sin\left(\frac{2\pi\omega_1}{\omega}\right) = 0$ and $\cos\left(\frac{2\pi\omega_1}{\omega}\right) = (-1)^n$. Finally, by using (B.8) and (B.9) in (2.21), we arrive at the formulas for $c_{\text{SN},1}$ and $c_{\text{PD},1}$ given in (3.15) and (3.16). \square

Proof of Proposition 3.3. With $p \geq 2$, the calculation of ξ_p is identical to that for $p = 1$, given above in the proof of Proposition 3.2, except corresponds to an evolution time of $\frac{z'-z+2\pi p}{\omega}$ instead of $\frac{z'-z+2\pi}{\omega}$. It follows that, instead of (B.6), we have

$$\xi_p = e^{-\frac{4\pi p\zeta}{\omega}} \left(\cos\left(\frac{2\pi p\omega_1}{\omega}\right) - \frac{\zeta}{\omega_1} \sin\left(\frac{2\pi p\omega_1}{\omega}\right) \right)^2 - e^{-\frac{2\pi p\zeta}{\omega}} \left(\cos\left(\frac{2\pi p\omega_1}{\omega}\right) - \frac{3\zeta}{\omega_1} \sin\left(\frac{2\pi p\omega_1}{\omega}\right) \right). \quad (\text{B.10})$$

At resonance, $\sin\left(\frac{2\pi p\omega_1}{\omega}\right) = \sin(\pi) = 0$ and $\cos\left(\frac{2\pi p\omega_1}{\omega}\right) = \cos(\pi) = -1$, so (B.10) reduces to

$$\xi_p = E_p(E_p + 1), \quad (\text{B.11})$$

where $E_p = e^{-\frac{2\pi p\zeta}{\omega}}$. Notice $E_p = \delta^{\frac{p}{2}}$, by (3.11), so by evaluating (2.24) we obtain

$$\begin{aligned} s_p^\pm &= (1 \pm E_p)(-\epsilon^2 E_p \mp 1) + (1 + \epsilon)^2 E_p \\ &= \mp(1 \mp \epsilon E_p)^2, \end{aligned} \quad (\text{B.12})$$

using also (3.7) and (3.8).

Next, $\kappa'_p = \frac{\partial \kappa_p}{\partial \omega}$, where $\kappa_p = \tau - 2\sqrt{\delta} \cos\left(\frac{\pi}{p}\right)$. So by using the formulas (3.11) for τ and δ , we obtain

$$\kappa'_p = \frac{4\pi}{\omega^2} e^{-\frac{2\pi\zeta}{\omega}} \left(\zeta \cos\left(\frac{2\pi\omega_1}{\omega}\right) + \omega_1 \sin\left(\frac{2\pi\omega_1}{\omega}\right) - \zeta \cos\left(\frac{\pi}{p}\right) \right).$$

At resonance, $\cos\left(\frac{2\pi\omega_1}{\omega}\right) = \cos\left(\frac{\pi}{p}\right)$ and $\sin\left(\frac{2\pi\omega_1}{\omega}\right) = \sin\left(\frac{\pi}{p}\right)$, so

$$\kappa'_p = \frac{4\pi\omega_1}{\omega^2} e^{-\frac{2\pi\zeta}{\omega}} \sin\left(\frac{\pi}{p}\right). \quad (\text{B.13})$$

Finally, by substituting (B.12) and (B.13) into (2.25), and further using the formulas listed in §3.3, we obtain after simplification $c_{\text{SN},p}$ and $c_{\text{PD},p}$ as given in (3.17). \square

References

- [1] Y. Liu, J. Páez Chávez, J. Zhang, J. Tian, B. Guo, and S. Prasad. The vibro-impact capsule system in millimeter scale: numerical optimisation and experimental verification. *Meccanica*, 55:1885–1902, 2020.
- [2] Y. Liu, M. Wiercigroch, E. Pavlovskaja, and H. Yu. Modelling of a vibro-impact capsule system. *Int. J. Mech. Sci.*, 66:2–11, 2013.

- [3] H. Dankowicz, X. Zhao, and S. Misra. Near-grazing dynamics in tapping-mode atomic-force microscopy. *Int. J. Non-Linear Mech.*, 42(4):697–709, 2007.
- [4] S. Misra, H. Dankowicz, and M.R. Paul. Degenerate discontinuity-induced bifurcations in tapping-mode. *Phys. D*, 239:33–43, 2010.
- [5] F. Chu and Z. Zhang. Bifurcation and chaos in a rub-impact Jeffcott rotor system. *J. Sound Vib.*, 210(1):1–18, 1998.
- [6] K. Mora, A. Champneys, A. Shaw, and M.I. Friswell. Explanation of the onset of bouncing cycles in isotropic rotor dynamics; a grazing bifurcation analysis. *Proc. R. Soc. A*, 476:20190549, 2020.
- [7] C.K. Halse, R.E. Wilson, M. di Bernardo, and M.E. Homer. Coexisting solutions and bifurcations in mechanical oscillations with backlash. *J. Sound Vib.*, 305:854–885, 2007.
- [8] S. Theodossiades and S. Natsiavas. Non-linear dynamics of gear-pair systems with periodic stiffness and backlash. *J. Sound Vib.*, 229(2):287–310, 2000.
- [9] P. Brzeski, A.S.E. Chong, M. Wiercigroch, and P. Perlikowski. Impact adding bifurcation in an autonomous hybrid dynamical model of a church bell. *Mech. Syst. Signal Process.*, 104:716–724, 2018.
- [10] J. Awrejcewicz and C. Lamarque. *Bifurcation and Chaos in Nonsmooth Mechanical Systems*. World Scientific, Singapore, 2003.
- [11] B. Blazejczyk-Okolewska, K. Czolczynski, T. Kapitaniak, and J. Wojewoda. *Chaotic Mechanics in Systems with Impacts and Friction*. World Scientific, Singapore, 1999.
- [12] R.A. Ibrahim. *Vibro-Impact Dynamics.*, volume 43 of *Lecture Notes in Applied and Computational Mechanics*. Springer, New York, 2009.
- [13] A.J. Van der Schaft and J.M. Schumacher. *An Introduction to Hybrid Dynamical Systems*. Springer-Verlag, New York, 2000.
- [14] W. Chin, E. Ott, H.E. Nusse, and C. Grebogi. Grazing bifurcations in impact oscillators. *Phys. Rev. E*, 50(6):4427–4450, 1994.
- [15] A.B. Nordmark. Non-periodic motion caused by grazing incidence in impact oscillators. *J. Sound Vib.*, 145(2):279–297, 1991.
- [16] A.P. Ivanov. Stabilization of an impact oscillator near grazing incidence owing to resonance. *J. Sound Vib.*, 162(3):562–565, 1993.
- [17] S. Foale. Analytical determination of bifurcations in an impact oscillator. *Proc. R. Soc. Lond. A*, 347:353–364, 1994.
- [18] F. Peterka. Bifurcations and transition phenomena in an impact oscillator. *Chaos Solitons Fractals*, 7(10):1635–1647, 1996.
- [19] S. Kundu, S. Banerjee, and D. Giaouris. Vanishing singularity in hard impacting systems. *Discrete Contin. Dyn. Syst. Ser B*, 16(1):319–332, 2011.
- [20] S. Kundu, S. Banerjee, J. Ing, E. Pavlovskaja, and M. Wiercigroch. Singularities in soft-impacting systems. *Phys. D*, 241:553–565, 2012.
- [21] H. Dankowicz and X. Zhao. Local analysis of co-dimension-one and co-dimension-two grazing bifurcations in impact microactuators. *Phys. D*, 202:238–257, 2005.

- [22] X. Zhao and H. Dankowicz. Unfolding degenerate grazing dynamics in impact actuators. *Nonlinearity*, 19(2):399–418, 2006.
- [23] J.F. Mason and P.T. Piiroinen. The effect of codimension-two bifurcations on the global dynamics of a gear model. *SIAM J. Appl. Dyn. Syst.*, 8(4):1694–1711, 2009.
- [24] H. Jiang, A.S.E. Chong, Y. Ueda, and M. Wiercigroch. Grazing-induced bifurcations in impact oscillators with elastic and rigid constraints. *Int. J. Mech. Sci.*, 127:204–214, 2017.
- [25] S. Yin, G. Wen, J. Ji, and H. Xu. Novel two-parameter dynamics of impact oscillators near degenerate grazing points. *Int. J. Non-Linear Mech.*, 120:103403, 2020.
- [26] A.B. Nordmark. Existence of periodic orbits in grazing bifurcations of impacting mechanical oscillators. *Nonlinearity*, 14:1517–1542, 2001.
- [27] P. Thota, X. Zhao, and H. Dankowicz. Co-dimension-two grazing bifurcations in single-degree-of-freedom impact oscillators. *J. Comput. Nonlinear Dynam.*, 1(4):328–335, 2006.
- [28] I. Ghosh and D.J.W. Simpson. The VIVID function for numerically continuing periodic orbits arising from grazing bifurcations of hybrid dynamical systems. <https://arxiv.org/abs/2510.16218>, 2025.
- [29] E. Pavlovskaja, J. Ing, M. Wiercigroch, and S. Banerjee. Complex dynamics of bilinear oscillator close to grazing. *Int. J. Bifurcation Chaos*, 20(11):3801–3817, 2010.
- [30] J. de Weger, D. Binks, J. Molenaar, and W. van de Water. Generic behavior of grazing impact oscillators. *Phys. Rev. Lett.*, 76(21):3951–3954, 1996.
- [31] P.T. Piiroinen, L.N. Virgin, and A.R. Champneys. Chaos and period-adding: Experimental and numerical verification of the grazing bifurcation. *J. Nonlin. Sci.*, 14(4):383–404, 2004.
- [32] J. Qiu and Z.C. Feng. Parameter dependence of the impact dynamics of thin plates. *Computers and Structures*, 75:491–506, 2000.
- [33] T. Witelski, L.N. Virgin, and C. George. A driven system of impacting pendulums: Experiments and simulations. *J. Sound Vib.*, 333:1734–1753, 2014.
- [34] J. Ing, E. Pavlovskaja, M. Wiercigroch, and S. Banerjee. Experimental study of impact oscillator with one-sided elastic constraint. *Phil. Trans. R. Soc. A*, 366:679–704, 2008.
- [35] J.D. Meiss. *Differential Dynamical Systems*. SIAM, Philadelphia, 2007.
- [36] J. Molenaar, J.G. de Weger, and W. van de Water. Mappings of grazing-impact oscillators. *Nonlinearity*, 14:301–321, 2001.
- [37] V.A. Dobrushkin. *Applied Differential Equations. The Primary Course*. CRC Press, Boca Raton, FL, 2015.
- [38] A.J. Homburg and B. Sandstede. Homoclinic and heteroclinic bifurcations in vector fields. In B. Hasselblatt, H.W. Broer, and F. Takens, editors, *Handbook of Dynamical Systems.*, volume 3, pages 379–524. Elsevier, New York, 2010.
- [39] A.J. Homburg, H. Kokubu, and V. Naudot. Homoclinic-doubling cascades. *Arch. Rational Mech. Anal.*, 160:195–243, 2001.
- [40] B.E. Oldeman, B. Krauskopf, and A.R. Champneys. Death of period-doublings: locating the homoclinic-doubling cascade. *Phys. D*, 146:100–120, 2000.
- [41] M. di Bernardo, C.J. Budd, A.R. Champneys, and P. Kowalczyk. *Piecewise-smooth Dynamical Systems. Theory and Applications*. Springer-Verlag, New York, 2008.